ELSEVIER

Journal of Organometallic Chemistry 648 (2002) 251–269

Journal of Organometallic Chemistry

www.elsevier.com/locate/jorganchem

Intramolecular interactions in 2,6-pyridylacetylenes and their $Co_2(CO)_4$dppm complexes

Bogdan H. Dana, Brian H. Robinson *, Jim Simpson

Department of Chemistry, University of Otago, P.O. Box 56, Dunedin, New Zealand

Received 28 September 2001; accepted 6 November 2001

Abstract

A series of 2,6-ethynylpyridyl compounds $BrC_5H_3N(C_2)R$, $C_5H_3N[(C_2)R]_2$, $BrC_5H_3N[RC_2Co_2(CO)_4dppm]$, $C_5H_3N\{[R'C_2Co_2(CO)_4dppm]C_2R\}$ and $C_5H_3N[(R_2C_2Co_2(CO)_4dppm)]_2$ ($R' = H$, $SiMe_3$, Fc), $C_5H_3N(C_2SiMe_3)(C_2R)$ $R = H$, Fc, $\{C_5H_3N(C_2SiMe_3)_2\}$ and $\{C_5H_3N[C_2C_5H_3N(C_2SiMe_3)]_2\}$ have been prepared in order to study through-space and through-bond interactions between the ethynyl arms. The structure of $BrC_5H_3N[FcC_2Co_2(CO)_4dppm]$ shows that the Co_2-alkyne unit is preferentially distorted, rather than the ethynyl arms bent, in order to minimise steric interactions. Although, there is no evidence for through-bond or through-space electronic communication between the redox centres, intramolecular interactions force a η^2(dppm)–η^1(dppm) equilibrium upon the oxidised $Co_2(CO)_4$dppm unit, which is seen in the electrochemistry and OTTLE data.

Keywords: Ethynylpyridyls; Redox; Intramolecular interactions; Carbonyl complexes; Ferrocenyl

1. Introduction

In simple arrays, energy transfer can be modulated by through-bond communication via an unsaturated link providing the orbital energy and phase are compatible. During our development of switchable organometallic fluorophores we have become aware that intramolecular through-space interactions can also play an important role. With some arrays containing ferrocenyl and carbonyl cluster redox centres, cofacial perturbation may be of greater significance than classical through-bond communication. We were interested in investigating if this is the case with 'aza' compounds. Bidentate *N*-donor ligands with alkyne functionality have been used extensively as building blocks for a wide range of molecular materials [1,2] but monodentate ethynylpyridyls have received less attention [3].

Of particular interest are 2,6-ethynylpyridyls with pendant –C≡C– arms as they have the correct orientation for through-space interactions. It has been argued by Okubo et al. [4] from MO calculations, and Novak et al. [4] from the He I and He II photoelectron spectra, that there is a weak intramolecular nitrogen lone pair-π'_{cc} (in-plane) through-space interaction in molecules in which the ethynyl group is adjacent to the nitrogen. These interactions manifest themselves in the relative energies of the π levels in 2- and 4-ethynylpyridines and the different intensities of the photoionisation bands. So, in principle, pendant redox centres of 2,6-ethynylpyridines should be able to communicate using the $n - \pi'_{cc}$ intramolecular route. On the other hand, coordination of a metal ion to the *N*-donor atom will be difficult, both from the reduced basicity and steric congestion, a feature noted by Butler [5] for analogous bipyridine compounds. This could be an advantage when constructing polyconjugated systems with useful semiconductor properties [6]. It is pertinent to note that while the –C≡C– bond has no role in the coordination of a metal ion to 1,2-bis(2-pyridyl)ethynes [7], it could be forced into that role with 2,6-ethynylpyridyls as templates. No complexes of 2- or 2,6-pyridylacetylenes where the –C≡C– bond has been used to coordinate a metal carbonyl unit have been reported, although 4- and 4,4′-pyridylacetylene [8] complexes are known.

In this paper, we report a series of 2,6-ethynylpyridyl organometallic compounds, with and without an ethynylferrocenyl substituent, and their complexes with

* Corresponding author. Fax: +64-3-4797906.
E-mail address: brobinson@alkali.otago.ac.nz (B.H. Robinson).

0022-328X/02/$ - see front matter
PII: S0022-328X(01)01426-7

the Co_2 electrophores, $C_2Co_2(CO)_6$ and $C_2Co_2(CO)_4$-dppm. The redox chemistry of these Co_2 redox centres is well-established, the former providing an unstable reduced species, whereas the latter usually gives a reversible oxidation couple [9,10]; communication between these redox centres has been demonstrated for several systems [11]. The parent 2,6-ethynylpyridine [4] and bis-2,6-(ethynylferrocenyl)pyridine [5] are the only reported 2,6-ethynyl derivatives so the series herein enabled their electronic structure and intramolecular interactions to be probed for the first time.

2. Results and discussion

The reaction between RC≡CH (R = Me_3Si, Fc) and 2,6-dibromopyridine under Sonogashira coupling conditions [12] gave reasonable yields of both the partially substituted 2,6-bromopyridylacetylenes **2**, **3** and fully substituted 2,6-pyridyldiacetylenes **5**, **6** (Scheme 1). Desilylation of **2** and **5** gave the parent ethynylpyridyls **1** and **4**, respectively. These red stable solids were characterised by microanalyses, ^{1}H-, ^{13}C-NMR and vibrational spectroscopy; ν(C≡C) occurred in the typical region at 2054 ± 1 cm^{-1}.

For our study of intramolecular interactions we needed a route to asymmetrically substituted 2,6-ethynylpyridyls and complexes which had a redox centre across the acetylene group. Both targets were accomplished by coordinating an oxidisable $Co_2(CO)_4$dppm unit. Thus, the reaction of **1**–**6** with $Co_2(CO)_6$dppm in benzene gave the respective complexes in which the Co_2 unit is coordinated either to one (**10**–**12**) or two (**15**–**17**) ethynyl arms. Complexes **9**, **13**, **14** with a reducible $Co_2(CO)_6$ unit, made for comparative electrochemical work, were also characterised. An indication of the steric restrictions for coordination came from the more severe conditions required to substitute **6** and the low yield. Microanalyses and spectroscopy were consistent with all formulae and the variable-temperature ^{31}P-NMR showed that there were no fluxional processes involving the $Co_2(CO)_4$dppm group on the NMR timescale.

Complex **11** provided the template for elaboration of the basic configuration to give molecules with asymmetric ethynyl substitution and two or three pyridyl rings (Scheme 2). By taking advantage of the preferential desilylation of a non-coordinated alkyne group, **11** was first converted to **18** to give a reactive ethynyl arm. A coupling reaction of **18** with iodoferrocene gave the asymmetric **19**. Self-coupling of **18** gave **20** which has a butadiyne link and terminating $Me_3Si_2C_2Co_2(CO)_4$-(dppm) groups. Reaction with 2,6-dibromopyridine gave the trimer **21**.

In order to obtain structural parameters for the 2,6-pyridyl framework a number of crystals were examined by X-ray diffraction. Remarkably, all but those for one compound, **8**, were extensively twinned. Complex **8** crystallises with two unique molecules in the orthorhombic unit cell. Small differences in bond lengths and angles between the discrete molecular units can be ascribed to crystal packing effects. Bond length and angle data from molecule 1 will be used in the ensuing discussion. Individual molecules are well separated with the closest intermolecular contact, not involving H atoms 1, 3.2939(8) Å between C(123) and O(261). A perspective view of one of the molecules is shown in Fig. 1, which defines the atom numbering scheme.

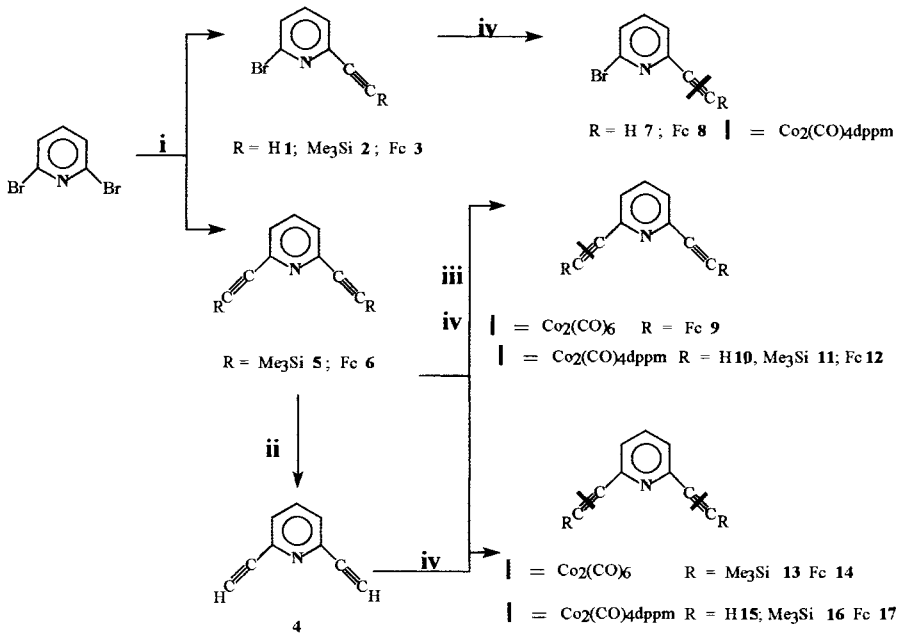

Scheme 1. (i) $Pd(PPh_3)_2Cl_2/CuI/^iPr_2NH$; (ii) K_2CO_3, MeOH; (iii) $Co_3(CO)_8$, benzene; (iv) $Co_2(CO)_6$dppm, benzene.

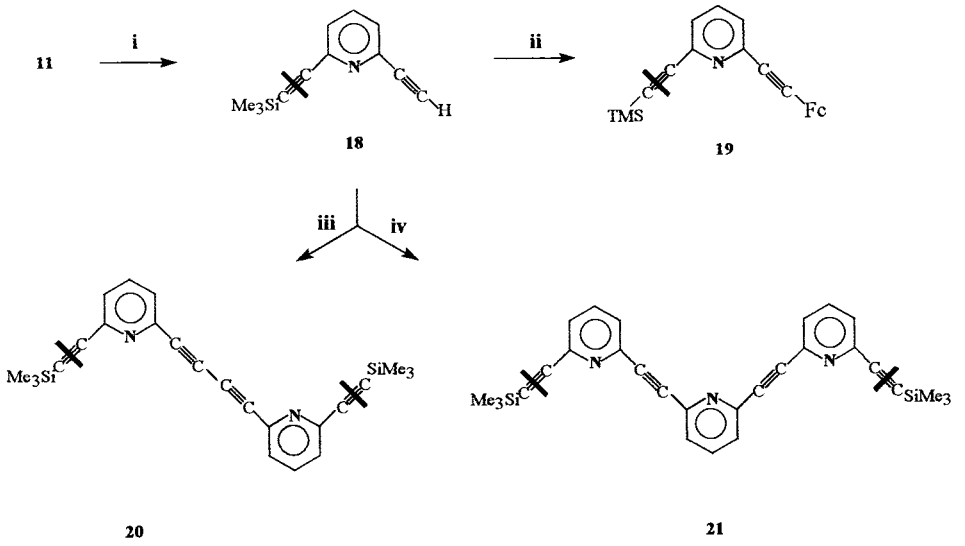

Scheme 2. (i) K_2CO_3, MeOH; (ii) $Pd(PPh_3)_2Cl_2$, CuI, $^iPr_2NH$; (iii) O_2, CuI; (iv) **3**, $Pd(PPh_3)_2Cl_2$, CuI, $^iPr_2NH = Co_2(CO)_4$dppm.

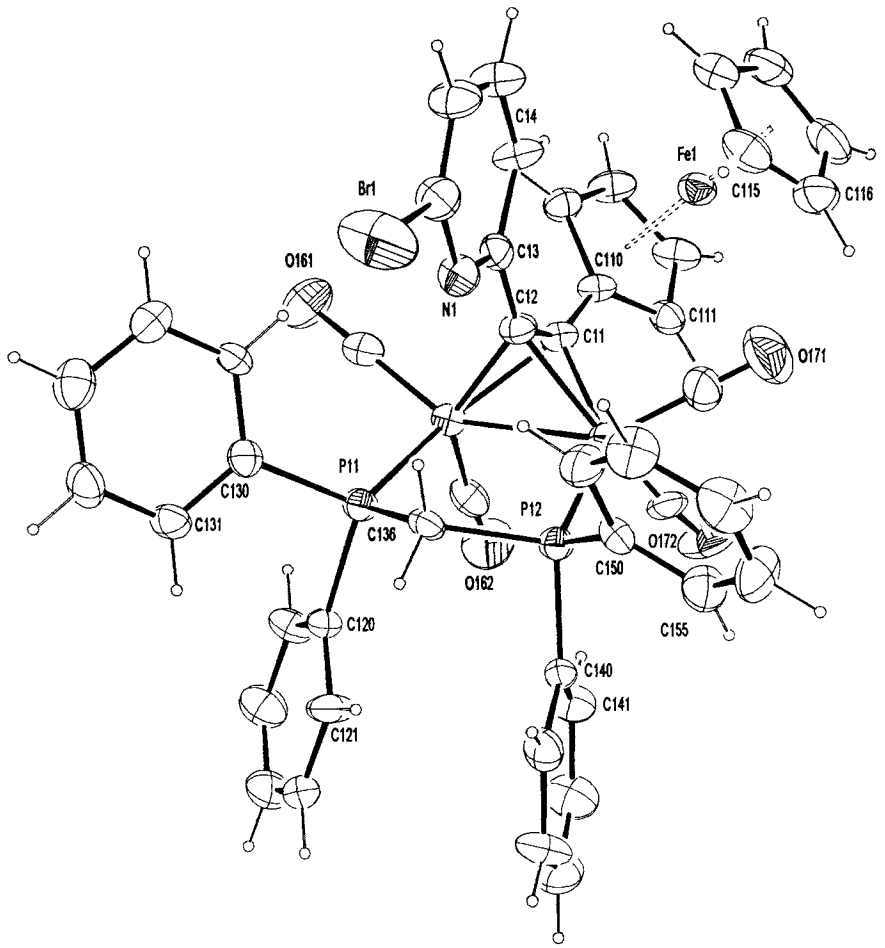

Fig. 1. Perspective view of molecule 1 of **8** showing the atom numbering scheme, with displacement ellipsoids drawn at the 50% probability level. For clarity only two C atoms of consecutively numbered cyclopentadienyl and phenyl rings and the O atoms of the carbonyl ligands have been labeled.

Table 1
Selected bond lengths (Å) and angles (°) for **8**

Bond lengths			
C(13)–C(14)	1.423(7)	Co(12)–C(12)	1.979(5)
C(14)–C(15)	1.400(7)	Co(11)–Co(12)	2.5059(11)
C(15)–C(16)	1.374(7)	Co(11)–P(11)	2.2612(19)
C(16)–C(17)	1.359(7)	Co(12)–P(12)	2.2416(17)
C(17)–Br(1)	1.910(6)	P(11)–C(136)	1.826(5)
C(17)–N(1)	1.335(6)	P(12)–C(136)	1.842(5)
C(13)–N(1)	1.359(6)	C(11)–C(110)	1.479(7)
C(12)–C(13)	1.450(7)	C(110)–C(111)	1.419(7)
C(11)–C(12)	1.338(7)	C(110)–C(114)	1.438(6)
Co(11)–C(11)	1.994(5)	C(111)–C(112)	1.425(7)
Co(11)–C(12)	1.969(6)	C(112)–C(113)	1.421(7)
Co(12)–C(11)	1.961(5)	C(113)–C(114)	1.411(7)
Bond angles			
C(11)–C(12)–C(13)	137.7(6)		
C(12)–C(11)–C(110)	146.4(5)		
C(11)–Co(11)–P(11)	140.62(16)		
C(12)–Co(11)–P(11)	104.01(18)		
C(11)–Co(12)–P(12)	140.66(17)		
C(12)–Co(12)–P(12)	105.59(18)		
P(11)–C(136)–P(12)	112.1(3)		
C(161)–Co(11)–Co(12)	150.79(18)		
C(171)–Co(12)–Co(11)	149.24(18)		

Selected bond length and angle data appear in Table 1. The molecule comprises an ca. tetrahedral (μ-alkyne)dicobalt core, typical of a perpendicular alkyne complex with an interline angle C(11–C(12)–Co(11)–Co(12) of 91.7(3)°. The alkyne carbon atoms carry ferrocenyl (C11) and 6-bromo-pyridyl substituents (C12), respectively in the normal *cis*-bent configuration. The large differences in the alkyne bend–back angles between the pyridyl substituent, C(13)–C(12)–C(11) 137.7(6)° and to the ferrocene, C(110)–C(11)–C(12) 146.4(5)°, suggests a requirement to minimise steric interactions between the (μ-alkyne)dicobalt and ferrocenyl residues. The ferrocenyl rings are ca. eclipsed and with the dihedral angle 2.6(5)° between the two Cp ring planes. The average Fe–C distance, 2.057(6) Å, is not unusual. The dppm ligand bridges the Co–Co bond of the (μ-alkyne)dicobalt moiety in a (μ-η^2) configuration with normal Co–P bond distances. These together with one 'axial' and one pseudo-equatorial CO ligand on each Co atom constitute the classical 'sawhorse' arrangement of ligands for the C_2Co_2 unit [13]. The dppm ligand binds on the same side of the C_2Co_2 moiety as the bromopyridyl substituent presumably to minimise intramolecular interactions with the more sterically demanding ferrocenyl group.

There is evidence of distortion of the quasi-tetrahedral C_2Co_2 unit with unequal Co–C bonds and an unusually long Co(11)–Co(12) bond, 2.5059(11) Å. The majority of (μ-alkyne)dicobalt complexes exhibit Co–Co bond distances in the range 2.46–2.47 Å [11,14,15], with such significant bond extension confined to complexes where two P-donor atoms chelate to a single Co atom [16] or when the core is chelated in a (μ-η^2) fashion by two bidentate phosphine [17] or arsine [18] ligands. A long Co–Co bond has been noted previously for the complex (dppm)$(CO)_4$-$Co_2C_2Fc_2C_2Co_2(CO)_4$(dppm) [14], where the effect was ascribed to steric interactions within the molecule. A similar explanation can be advanced for **8**. It would appear that the molecule distorts the Co_2 unit rather than bending back the ethynyl arms to accommodate the bulky $Co_2(CO)_4$(dppm). This is energetically easier given that the ethynyl→Co_2 orbital configuration is relatively flexible and a slight twist of the alkyne axis or lengthening of the Co–Co bond has little effect on the potential energy profile.

2.1. Redox chemistry

All molecules containing one or more redox centre were investigated by electrochemical techniques with all potentials referenced against decamethylferrocene (Table 2); OTTLE methods were also employed where there were two redox centres.

A single reversible one- or two-electron process was observed in the cyclic and square wave voltammograms for the ferrocenyl compounds **3** and **6**, respectively. $E^{+/0}$[Fc] for **6** (0.62 V) was similar to that for ethynylferrocene (0.61 V), whereas the inductive effect of the electronegative bromine substituent on the pyridyl ring causes this to increase in **3** (0.71 V). The UV–vis of

Table 2
Electrochemical data [a]

	E^0[Fc]$^{+/0}$	$[Co_2]^{+/0}$ [b]		
		E_a(**A**)	E_c(**A′**)	E_a(**B**)
3	0.71			
6	0.65			
7		0.81	0.74	
8	0.50	1.02		
9	0.80, 0.91			
10		0.65		
11		0.69		
12	0.64, 0.75	[c]		
14	0.60			
15		0.80	0.64	0.97
16		0.69	0.59	0.77
17	0.48	1.06	0.91	
18		0.80	0.65	
19	0.70	1.3		1.65
20		0.81	0.61	1.05
21		0.65		

[a] In volts, referenced to decamethylferrocene ($E^{+/0}$ (ethynylferrocene) = 0.61, ferrocene 0.55 V); CH_2Cl_2, scan rate 200 mV s^{-1}.
[b] (**A**) and (**B**) refer to the two processes as defined in the text.
[c] Not observed.

$\mathbf{6}^{2+}$ had the typical ferrocenium $e_2'' \rightarrow$ LUMO absorption [19] at 610 nm but no bands of lower energy which often [20] characterise interacting ferrocenyls linked by an ethynyl group. These data indicate that there is no through-bond communication between the two ferrocenyl redox centres in **6** even though the orbital phases for a $Fc-n-\pi_{cc}-Fc$ interaction are correct and symmetry allowed. This conclusion was also reached [21] for the analogous arene compound 1,3-bis(ethynyl)-benzene **22**. The difference between **6** and **22** is that the latter has symmetry mismatch which forbids any interaction [22]. In contrast, the cofacially-orientated 1,2-bis-(ethynyl)benzene **23** has two one-electron processes in the cyclic voltammograms [21] indicative of communication, through-space interaction having a larger role in this instance.

The situation is more complex for those complexes that have a C_2Co_2dppm [Co_2] redox centre. Previous work has shown [9–11] that $E^{+/0}$[Co_2] for an isolated $(Me_3Si)_2C_2Co_2(CO)_4$dppm redox centre is 0.67 V. Due to the electrostatic effect of a Fc^+ substituent, this increases to $\sim$1.1 V in $Fc_2C_2Co_2(CO)_4$dppm; $E^{+/0}$-[Fc] = 0.49 V. Comparable data for $Fc_2C_2Co_2(CO)_6$ are $E^{+/0}$[Fc] = 0.64 V and $E^{+/0}$[Co_2] = −1.3 V. Electrochemical assignments for the pyridyl complexes with a ferrocenyl substituent, **8**, **9**, **12**, **14**, **17**, **19**, readily follow from these reference data (Table 2). It is clear that, despite the close proximity of the ethynyl arms, the ferrocenyl redox orbitals are not usually perturbed by through-pyridyl or through-space interactions and act independently of the other ethynyl arm. The exception may be **19** where both $E^{+/0}$[Fc] and $E^{+/0}$[Co_2] are significantly higher than in comparable complexes, which may be the result of unfavourable intramolecular interactions and the lability of the dppm upon oxidation (see below).

If the ferrocenyl and cobalt-centred redox centres were to act independently, as is the case in other systems [11,14], through-space interactions may be reflected in the $[Co_2]^{+/0}$ couple. However, in contrast to the behaviour of most $R_2C_2Co_2(CO)_4$dppm complexes [9–11], the i/V responses of the $[Co_2]^{+/0}$ couple for the 2,6-pyridyl complexes display a marked temperature, scan rate and solvent dependence in the electrochemical parameters. The chemical reversibility depends on the type of substituent on the ethynyl arm. For this reason both the anodic and cathodic potentials for the oxidation of the $Co_2(CO)_4$dppm units are quoted in Table 2; $E_a - E_c$ values for the i/V scans were characteristically large and the system is kinetically rather than diffusion-controlled. In general, the $[Co_2]^{+/0}$ potentials for the 2,6-pyridyl complexes are similar to those of other $Co_2(CO)_4$dppm complexes without a pyridyl backbone. The slight increase in potential could be ascribed to the weak $n-\pi'_{cc}$ interaction. The $[Co_2]^{+/0}$ couple for **12** was not observed, either because it was forced outside the scan range by the electrostatic effect of two Fc^+ groups or the dppm ligand is lost upon oxidation.

Given that the crystal structure indicates that the Co_2 unit is distorted, it is logical to look to the lability of the dppm to account for the non-reversible and variable electrochemical behaviour. Complexes with two $Co_2(CO)_4$dppm units, **15** and **16**, provided an insight into the mechanism. The cyclic voltammogram of **15** at 200 mV s^{-1}, whether at a platinum disk electrode or in an OTTLE cell, shows (Fig. 2a) two anodic waves at $E_a = 0.80$ V (**A**) and 0.97 V (**B**) and a single cathodic wave $E_c = 0$ 64 V (**A′**).

Scan rate and temperature dependence of the $i_{(A)}-i_{(B)}$ ratio were indicative of an ECE process. When the scan was switched just past **A** the characteristic 'crossover' feature appeared (Fig. 2b). Previous work [11,23] has shown that the separation in E_a between the η^2- and η^1-dppm coordination in a $Co_2(CO)_x$ unit is $\sim$0.2 V, consistent with an assignment of E_a(**A**) and E_a(**B**) to oxidation of η^2-**15** and an 'unclipped' η^1-**15**, respectively. OTTLE data (Fig. 3) support this assignment. Oxidation up to E(**A**) generates a mixed spectrum of $[\eta^2$-**15**$]^+$ and a new species with ν(CO) at 2035, 2016, 1985 cm^{-1} that is similar to ν(CO) for $Ph_2C_2Co_2(CO)_5(\eta^1$-dppe) [23]. When the potential is decreased back to zero only the new species $[\eta^1$-**15**$]^0$ remains. A square scheme can be written for the sequence of electron transfer and the $\eta^2 \rightarrow \eta^1$ conversion (Scheme 3). Oxidation at **A** of $[\eta^2$-**15**$]^0$ leads to fast unclipping of the dppm to give $[\eta^1$-**15**$]^+$ which at potentials $<$ E(**B**) will be reduced to $[\eta^1$-**15**$]^0$. Because E(η^2-**15**) is $<$ E(η^1-**15**), $[\eta^1$-**15**$]^0$ will also be oxidised by $[\eta^2$-**15**$]^+$ in a cross electron transfer reaction. There is a vacant coordination site in η^1-**15**, a feature not uncommon [24] in ETC processes involving metal carbonyls. The extensive intramolecular interactions provide protection for the 16-electron cobalt atom.

This ECE mechanism is driven by the strong intermolecular interactions in the 2,6-pyridyl complexes and the kinetic parameters will obviously depend on the ethynyl substituents. This correlates well with the observation that i_a(**B**) is very small or non-existent for the monosubstituted complexes **7**–**12** and **18**–**21**. An interesting circumstance occurs with complexes with maximum congestion, **16** and **17**. OTTLE experiments with **16** show that at room temperature in CH_2Cl_2 only a small concentration of [η^1-**16**] is formed from $[\eta^2$-**16**$]^+$ at the electrode surface; that is, k_1 is small. Furthermore, k_2 is also small because of the congestion so that in the i/V scans anodic and cathodic components of **A** and **B** are seen (Fig. 4). Because of the slow 'unclipping' of dppm the profiles of the i/V scans for **16** are very dependent on the combination of scan rate, solvent and temperature dependent. For example, in MeCN, at

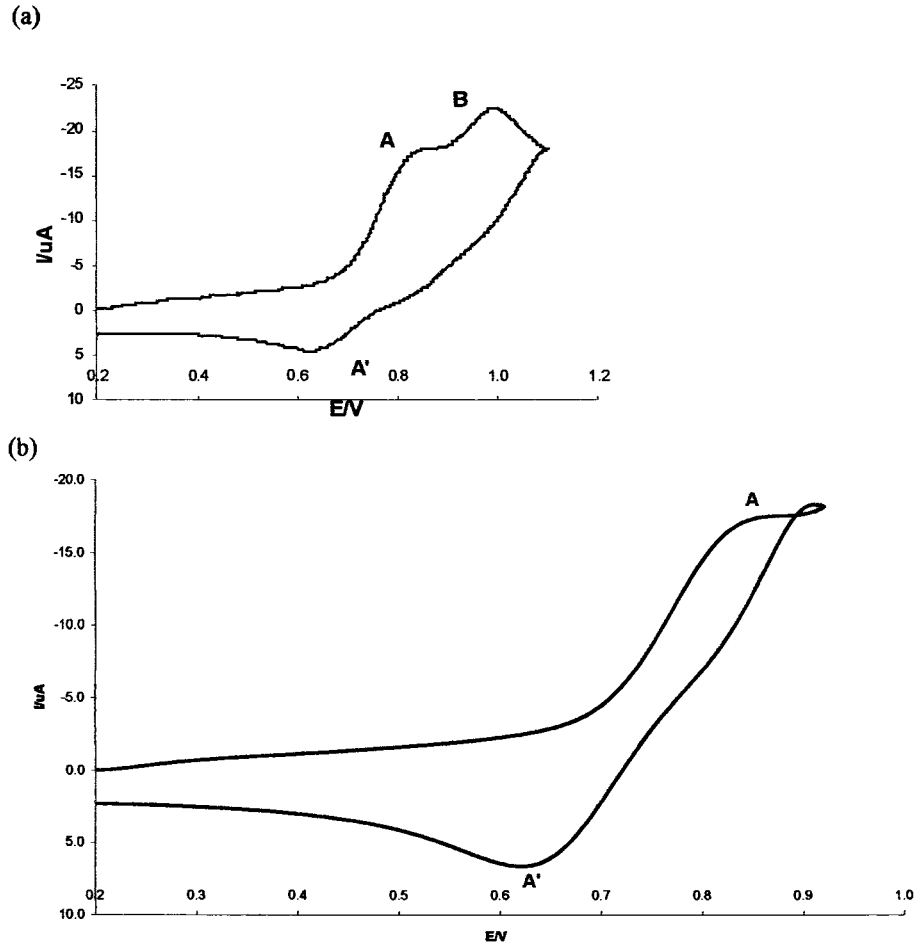

Fig. 2. Cyclic voltammograms of 15 in; CH_2Cl_2, Pt, $TBAPF_6$; 0.1 mol l^{-1}, 20 °C: (a) 0–1.1 V; (b) 0–0.88 V.

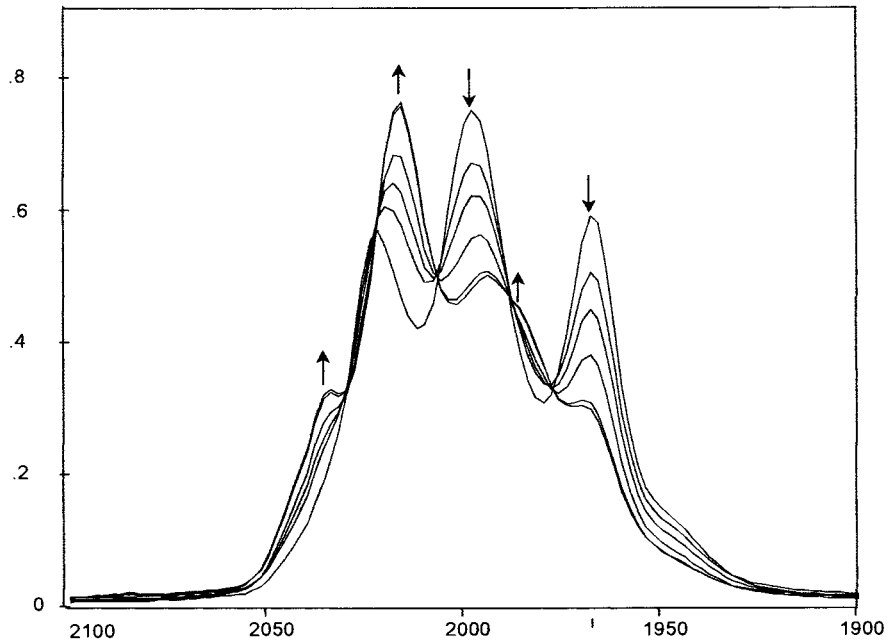

Fig. 3. OTTLE n(CO) scans of 15 for the sequence $0 \ll 1.0$ V; CH_2Cl_2; Pt, $TBAPF_6$; 0.1 mol l^{-1}. — refers to emerging h1-15 and ··· to the parent h2-15 species.

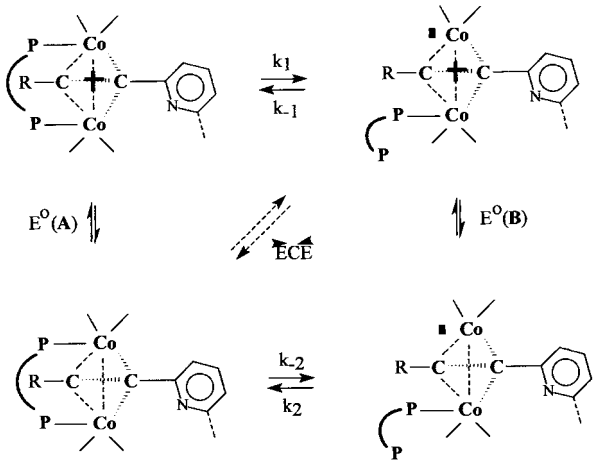

Scheme 3. ■ is a vacant coordination site.

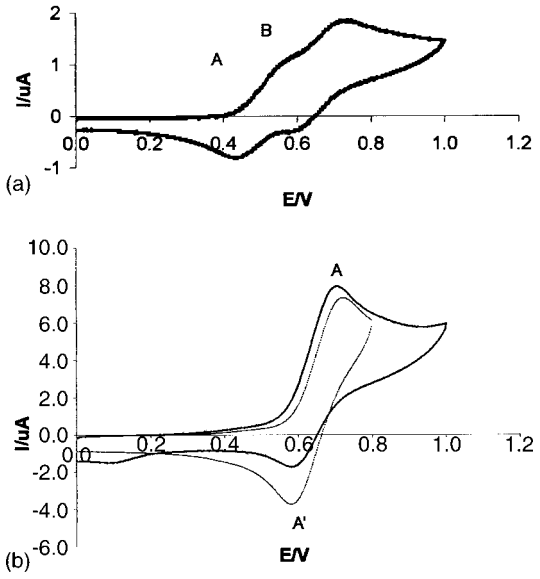

Fig. 4. Cyclic voltammograms of 16 Pt, $TBAPF_6$; 0.1 mol l^{-1}: (a) in CH_2Cl_2, 20 °C, 200 mV s^{-1}; (b) in MeCN, – 293 K, ----- 253 K, 800 mV s^{-1}.

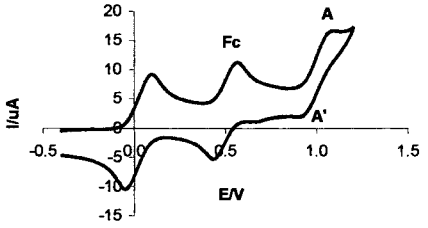

Fig. 5. Cyclic voltammogram of 17 in CH_2Cl_2; 400 mV s^{-1}, Pt, TBAPF6 0.1 mol l^{-1}, 20 °C; figure includes decamethylferrocene reference.

ambient temperatures, the electrochemistry and OTTLE data indicate that a [η^1-**16**] species is formed, with a solvent molecule in the vacant coordination site. However, at low temperatures in MeCN the $\eta^2 \leftrightarrow \eta^1$ interconversion is now slow such that a two-electron chemically quasi-reversible process for **A** ($i_c/i_a = 0.9$ at 1000 mV s^{-1}) is observed (Fig. 4b).

The most sterically congested environment is found in **17** and it is not surprising that the $[Co_2]^{+/0}$ couple is a two-electron reversible process under all conditions (Fig. 5).

3. Conclusion

While there is no orbital restriction on a RC≡C – $n - \pi'_{cc}$ – C≡CR through-bond interaction in 2,6-ethynylpyridyls the electrochemical and OTTLE data show that no significant interaction exists. Nevertheless, there are severe intramolecular interactions. Although, there is no evidence for through-space communication, such interactions are manifested in the distortions which occur in the solid state structure of **8** and the lability of the dppm in the oxidised $Co_2(CO)_4$dppm species. We have also found that only two 2,6-pyridyl ligands can coordinate to Cu(I) [20]. The 2,6-pyridyl unit therefore acts as a sterically congested node. These results contrast with those where the 2,6-ethynylpyridyl unit is incorporated into a σ-Pt backbone [3]. In these compounds, when quaternised, there was evidence for π-delocalisation and reasonable fluorescence and quantum yields.

4. Experimental

Solvents were dried and distilled by standard procedures, and all reactions were performed under N_2. Ethynylferrocene [25] and $Co_2(CO)_6$dppm [26] were prepared by literature methods. All other reagents were used as received from commercial sources. IR spectra were recorded on a Perkin–Elmer Spectrum BX FT–IR, NMR on a Varian VXR300 MHz and electronic spectra on a Jasco V 550. Microanalyses were carried out by the Campbell Microanalytical Laboratory, University of Otago. Mass spectra were recorded on a Kratos MS80RFA instrument with an Iontech ZN11NF atom gun. Cyclic and square wave voltammetry in CH_2Cl_2 were performed for all compounds using a three-electrode cell with a polished disk, Pt (2.27 mm^2) as the working electrode; solutions were $\sim 10^{-3}$ M in electroactive material and 0.10 M in supporting electrolyte (triply-recrystallised $TBAPF_6$). Data was recorded on an ADInstruments Powerlab 4SP computer-controlled potentiostat. Scan rates of 0.05–1 V s^{-1} were typically employed for cyclic voltammetry and for Osteryoung square-wave voltammetry, square-wave step heights of 1–5 mV, a square amplitude of 15–25 mV with a frequency of 30–240 Hz. All potentials are referenced to decamethylferrocene; $E_{1/2}$ for sublimed

ferrocene was 0.55 V. Infrared and UV–vis OTTLE data were obtained from standard cells with platinum grid electrodes.

4.1. Preparation of **2** and **5**

2,6-Dibromopyridine (2.00 g, 8.44 mol), bis(triphenylphosphine)palladium dichloride (0.35 g, 0.50 mmol) and copper(I) iodide (0.20 g, 1 mmol) were stirred in diisopropylamine (40 ml) for 30 min at room temperature (r.t.). Trimethylsilylacetylene (2.40 ml, 17.1 mmol) was then added dropwise to the reaction mixture, which was stirred for 3 h and then heated under reflux for 1 h. The volatiles were removed in vacuo and the brown solid obtained washed with water (3×30 ml), extracted with CH_2Cl_2 (2×50 ml), dried (over $MgSO_4$) and concentrated under reduced pressure. The residue was separated on silica gel, eluent 1:1 C_6H_{14}–CH_2Cl_2. Workup of band 1 gave **5** as a yellow powder (32% yield). Calc. for $C_{15}H_{21}NSi_2$: C, 66.42; H, 7.74; N, 5.16. Found: C, 66.15; H, 7.75; N, 5.18%. ^{1}H-NMR ($CDCl_3$): δ, 0.25 (s, 18H, $-CH_3$), 7.38 (d, 2H, Ar–H), 7.60 (t, 1H, Ar–H). ^{13}C-NMR ($CDCl_3$): δ, 143.35, 136.27, 126.68 (pyridine), 103.12, 95.43 (–C≡C–), 0.32 ($-CH_3$). IR (CH_2Cl_2, cm^{-1}): 2055 ($\nu_{C\equiv C}$).

Workup of band 2 gave **2** as a beige powder (1.15 g, 31% yield). Calc. for $C_{10}H_{12}BrNSi$: C, 47.24; H, 4.72; Br, 31.49; N, 5.51. Found: C, 47.63; H, 4.52; Br, 31.78; N, 5.61%. ^{1}H-NMR ($CDCl_3$): δ, 0.24 (s, 9H, $-CH_3$), 7.34 (d, 1H, Ar–H), 7.41 (d, 1H, Ar–H), 7.46 (t, 1H, Ar–H). IR (CH_2Cl_2, cm^{-1}): 2054 ($\nu_{C\equiv C}$).

4.2. Preparation of **1** and **4**

Complex **2** (1.15 g, 4.52 mmol) was stirred in MeOH (40 ml) with anhydrous K_2CO_3 (2.5 g, 18.1 mmol) for 72 h at ambient temperature. The crude reaction mixture was passed through a short pad of alumina and workup on silica gel, eluent 1:2 CH_2Cl_2–C_6H_{14} gave **1** as a pale yellow solid (0.25 g, 29%). Calc. for C_7H_4BrN: C, 46.15; H, 2.19; Br, 43.95; N, 7.69. Found: C, 46.50; H, 2.17; Br, 43.58; N, 7.33%. ^{1}H-NMR ($CDCl_3$): δ, 3.20 (s, 1H, ≡H), 7.43 (d, 1H, Ar–H), 7.46 (d, 1H, Ar–H), 7.51 (t, 1H, Ar–H). IR (CH_2Cl_2, cm^{-1}): 2054 ($\nu_{C\equiv C}$).

The reaction mixture from a similar reaction with **5** (0.15 g, 0.55 mmol) was quenched with water (50 ml) and extracted with CH_2Cl_2 (3×50 ml). The organic layers were dried over $MgSO_4$, passed through a short pad of neutral alumina and concentrated under reduced pressure to give **4** as a brown solid (0.06 g, 85%). Calc. for C_9H_5N: C, 85.04; H, 3.93; N, 11.02. Found: C, 84.91; H, 4.08; N, 10.75%. ^{1}H-NMR ($CDCl_3$): δ, 3.18 (s, 2H, ≡H), 7.46 (d, 2H, Ar–H), 7.62 (t, 1H, Ar–H). IR (CH_2Cl_2, cm^{-1}): 2054 ($\nu_{C\equiv C}$).

4.3. Preparation of **3** and **6**

A mixture of 2,6-dibromopyridine (0.20 g, 0.84 mmol) and ferrocenylacetylene (0.40 g, 1.94 mmol), bis(triphenylphosphine)palladium dichloride (30 mg, 43 μmol) and copper(I) iodide (31 mg, 162 μmol) in diisopropylamine (20 ml) was stirred under N_2 for 20 h at r.t. The crude reaction solution was treated with 30 ml each of water and CH_2Cl_2. The organic layer was separated and the aq. layer further extracted with two portions of CH_2Cl_2. The combined, dried ($MgSO_4$) organic phase was washed through a short neutral alumina column and the solvent stripped under reduced pressure. The residue was separated on silica gel, eluent 2:1 C_6H_{14}–CH_2Cl_2. Band 2 was removed and workup gave **4** as an orange powder (150 mg, 33%). Calc. for $C_{17}H_{12}BrFeN$: C, 55.73; H, 3.26; N, 3.82. Found: C, 56.19; H, 3.36; N, 3.73%. ^{1}H-NMR ($CDCl_3$): δ, 4.25 (s, 5H, $-C_5H_5Fe$), 4.29 (t, 2H, α-C_5H_5), 4.55 (t, 4H, β-C_5H_5), 7.40 (d, 2H, Ar–H), 7.55 (t, 1H, Ar–H). IR (CH_2Cl_2, cm^{-1}): 2055 ($\nu_{C\equiv C}$).

Band 3 gave **6** as an orange powder (50 mg, 12%). Calc. for $C_{29}H_{21}Fe_2N$: C, 70.30; H, 4.24; N, 2.82. Found: C, 69.85; H, 4.46; N, 2.63%. ^{1}H-NMR($CDCl_3$): δ, 4.26 (s, 10H, $-C_5H_5Fe$), 4.29 (t, 4H, α-C_5H_5), 4.57 (t, 4H, β-C_5H_5), 7.38 (d, 2H, Ar–H), 7.66 (t, 1H, Ar–H). IR (CH_2Cl_2, cm^{-1}): 2055 ($\nu_{C\equiv C}$).

4.4. Dppm complexes

4.4.1. Complex **7**

A mixture of **1** (35 mg, 193 μmol) and $Co_2(CO)_6$-dppm (257 mg, 385 μmol) was stirred at r.t. for 6 h in 30 ml of CH_2Cl_2. Workup on silica gel, eluent 9:1 CH_2Cl_2–MeOH gave **7** as a red solid (35 mg, 23%). Calc. for $C_{36}H_{26}BrCo_2NO_4P_2$: C, 54.27; H, 3.26; Br, 10.05; N, 1.75. Found: C, 54.01; H, 3.58; Br, 9.83; N, 1.91%. ^{1}H-NMR ($CDCl_3$): δ, 3.45 (q, 1H, $-CH_2$), 4.25 (q, 1H, $-CH_2$), 6.19 (s, 1H, α cluster-H), 6.80–7.50 (m, 23H, Py– and Ar–H). IR (CH_2Cl_2, cm^{-1}): 2025, 1997, 1968 (ν_{CO}). ^{31}P-NMR ($CDCl_3$): δ, 40.92.

4.4.2. Complex **8**

A mixture of **3**, (25 mg, 50.5 μmol) and $Co_2(CO)_6$-dppm (85 mg, 127 μmol) was heated under reflux for 3 h in 30 ml of CH_2Cl_2. Workup on silica gel, eluent 1:1 C_6C_{14}–CH_2Cl_2 gave **8** as a brown solid (30 mg, 35%). Calc. for $C_{46}H_{34}BrCo_2FeNO_4P_2$: C, 56.32; H, 3.46; N, 1.42. Found: C, 56.26; H, 3.65; N, 1.08%. ^{1}H-NMR ($CDCl_3$): δ, 3.20 (q, 2H, $-CH_2$), 4.10 (s, 10H, $-C_5H_5$), 4.32 (t, 4H, α-C_5H_5), 4.51 (t, 4H, β-C_5H_5), 5.2 (q, 2H, $-CH_2$), 7.05–7.50(m, 40H, Ar–H). IR (CH_2Cl_2, cm^{-1}): 2023, 1995, 1968 (ν_{CO}). ^{31}P-NMR ($CDCl_3$): δ, 38.49.

4.4.3. Complex **10**/**15**

A mixture of **4** (26 mg, 0.2 mmol) and $Co_2(CO)_6$dppm (0.34 g, 0.51 mmol) was stirred at r.t.

for 48 h in 30 ml of C_6H_6. Workup gave **10** as a brown solid (48 mg, 31%). Calc. for $C_{38}H_{27}Co_2NO_4P_2$: C, 61.37; H, 3.63; N, 1.88. Found: C, 61.33; H, 3.84; N, 1.89%. ^{1}H-NMR ($CDCl_3$): δ, 3.18 (s, 1H, -≡-H), 3.50 (m, 1H, $-CH_2$), 5.20 (m, 1H, $-CH_2$), 6.17 (s, 1H, -cluster-H), 7.36 (d, 2H, Ar–H), 7.45 (t, 1H, Ar–H). IR (CH_2Cl_2, cm^{-1}): 2025, 1997, 1970 (ν_{CO}), 2054 ($\nu_{C\equiv C}$).

From a similar reaction **4** (30 mg, 0.23 mmol)) and $Co_2(CO)_6$dppm (0.5 g, 0.74 mmol) was obtained **15** as a brown–red solid (150 mg, 47%). Calc. for $C_{67}H_{49}Co_4NO_8P_4$: C, 60.22; H, 3.67; N, 1.05. Found: C, 59.80; H, 4.39; N, 1.08%. ^{1}H-NMR ($CDCl_3$): δ (ppm) 3.50 (m, 1H, $-CH_2$), 4.2 (m, 1H, $-CH_2$), 6.20 (s, 1H, -cluster-H), 6.90–7.45 (m, 20H, Ar–H). ^{31}P-NMR ($CDCl_3$): δ, 42.34. IR (CH_2Cl_2, cm^{-1}): 2024, 1996, 1968 (ν_{CO}).

4.4.4. Complex **11**/**16**

A mixture of **5** (0.19 g, 0.7 mmol) and $Co_2(CO)_6$dppm (1.17 g, 1.75 mmol) was heated under reflux in C_6H_6 (50 ml) for 2 h. Workup of the first band using 1/1 C_6H_{14}–CH_2Cl_2 gave **11** as a brown solid (0.35 g, 57%). Calc. for $C_{44}H_{43}Co_2NO_4P_2Si_2$: C, 59.66; H, 4.85; N, 1.58. Found: C, 59.61; H, 4.88; N, 1.68%. EIMS (m/z): [MH$^+$] 886, [M$^+$ − CO] 857. ^{1}H-NMR ($CDCl_3$): δ, 0.39 (s, 18H, $-CH_3$), 3.20 (q, 2H, $-CH_2$), 5.10 (q, 2H, $-CH_2$), 6.92 (m, 8H, Ar–H), 7.23(s, 16H, Ar–H), 7.37 (t, 18H, Ar–H). ^{31}P-NMR ($CDCl_3$): δ, 37.44 ppm. IR (CH_2Cl_2, cm^{-1}): 2017, 1992, 1969 (ν_{CO}), 2055 ($\nu_{C\equiv C}$). $E_{1/2}$ (CH_2Cl_2): 0.60 V. The second band gave **16** as a dark brown solid (0.1 g, 11%). Calc. for $C_{73}H_{65}Co_4NO_8P_4Si_2$: C, 58.45; H, 4.37; N, 0.93. Found: C, 58.04; H, 4.92; N, 1.19%. EIMS (m/z): [MH$^+$] 1501. ^{1}H-NMR ($CDCl_3$): δ, 0.39 (s, 18H, $-CH_3$), 3.20 (q, 2H, $-CH_2$), 5.10 (q, 2H, $-CH_2$), 6.92 (m, 8H, Ar–H), 7.23 (s, 16H, Ar–H), 7.37 (t, 18H, Ar–H). IR (CH_2Cl_2, cm^{-1}): 1964, 1994, 2020 (ν_{CO}), 2058 ($\nu_{C\equiv C}$).

4.4.5. Complex **12**/**17**

A mixture of **6** (45 mg, 91 μmol) and $Co_2(CO)_6$dppm (270 mg, 403 μmol) was heated at reflux for 6 h in 40 ml of CH_2Cl_2. A dark red solid, obtained on removal of solvent was separated on silica gel, eluent 1:2 CH_2Cl_2–C_6H_{14}. Workup of band 1 gave **12** as a red solid (31%). Calc. for $C_{58}H_{43}Co_2Fe_2NO_4P_2$: C, 62.76; H, 3.87; N, 1.26. Found: C, 62.25; H, 4.23; N, 0.91%. ^{1}H-NMR ($CDCl_3$): δ, 3.45 (q, 1H, $-CH_2$), 4.25 (q, 1H, $-CH_2$), 4.05 (s, 5H, $-C_5H_5$), 4.12 (s, 5H, $-C_5H_5$), 4.30 (t, 2H, α-C_5H_5), 4.42 (t, 2H, α-C_5H_5), 4.55 (t, 2H, β-C_5H_5), 6.80–7.50 (m, 23H, Py– and Ar–H). IR (CH_2Cl_2, cm^{-1}): 2021, 1994, 1968 (ν_{CO}), 2054($\nu_{C\equiv C}$). ^{31}P-NMR ($CDCl_3$): δ, 39.20. Workup of band 2 gave red **17** (20%). Calc. for $C_{87}H_{65}Co_4Fe_2NO_8P_4$: C, 60.38; H, 3.75; N, 0.80. Found: C, 59.84; H, 3.70; N, 0.67%. ^{1}H-NMR ($CDCl_3$): δ, 3.45 (q, 1H, $-CH_2$), 4.25 (q, 1H, $-CH_2$), 6.19 (s, 1H, α cluster-H), 6.80–7.50 (m, 23H, Py– and Ph–H). IR (CH_2Cl_2, cm^{-1}): 2022, 1994, 1968 (ν_{CO}). ^{31}P-NMR ($CDCl_3$): δ, 42.80.

4.5. Preparation of $Co_2(CO)_6$ complexes

4.5.1. Complex **9**

A similar procedure using **6** (30 mg, 61 μmol) and $Co_2(CO)_8$ (27 mg, 79 μmol) gave green **9** (25 mg, 38%). Calc. for $C_{35}H_{21}Co_2Fe_2NO_6$: C, 53.77; H, 2.68; N, 1.79. Found: C, 53.42; H, 2.75; N, 1.66%. ^{1}H-NMR ($CDCl_3$): δ, 4.02 (s, 10H, $-C_5H_5$), 4.28 (t, 4H, $-\alpha C_5H_5$), 4.49 (t, 4H, $-\beta C_5H_5$), 7.60–7.80 (m, 3H, Py–H). IR (CH_2Cl_2, cm^{-1}): 2090, 2053, 2024 (ν_{CO}), 2212($\nu_{\equiv}$).

4.5.2. Complex **13**

Complex **5** (0.1 g, 0.37 mmol) and dicobaltoctacarbonyl (0.3 g, 0.98 mmol) were stirred in C_6H_6 (30 ml) for 6 h, at r.t. The volatiles were then removed under reduced pressure and the dark-red solid separated on silica gel, eluent 3:1 C_6H_{14}–CH_2Cl_2. The first major

Table 3
Crystal data and structure refinement for **8**

Empirical formula	$C_{92}H_{68}Br_2Co_4Fe_2N_2O_8P_4$
Formula weight	1960.60
Temperature (K)	168(2)
Wavelength (Å)	0.71073
Crystal system	Orthorhombic
Space group	*Pca*2(1)
Unit cell dimensions	
a (Å)	22.006(7)
b (Å)	12.158(4)
c (Å)	30.951(10)
α (°)	90
β (°)	90
γ (°)	90
V (Å^3)	8281(5)
Z	4
D_{calc} (mg m^{-3})	1.573
Absorption coefficient (mm^{-1})	2.225
F(000)	3952
Crystal size (mm^3)	0.43 × 0.16 × 0.11
Theta range for data collection (°)	2.02–26.41
Index ranges	$-14 \le h \le 27$, $-14 \le k \le 15$, $-38 \le l \le 38$
Reflections collected	102 993
Independent reflections	16 630 [$R_{int} = 0.0960$]
Completeness to theta = 26.41°	98.1%
Absorption correction	Empirical
Max/min transmission	1.000000, 0.888041
Refinement method	Full-matrix least-squares on F^2
Data/restraints/parameters	16 630/1/1028
Final *R* indices [$I > 2\sigma(I)$]	$R_1 = 0.0395$, $wR_2 = 0.0624$
R indices (all data)	$R_1 = 0.0904$, $wR_2 = 0.0712$
Absolute structure parameter	0.406(7)
Goodness-of-fit on F^2	0.847
Largest difference peak and hole (e Å^{-3})	0.992 and −0.842

Table 4
Atomic coordinates ($\times 10^4$) and equivalent isotropic displacement parameters ($Å^2 \times 10^3$) for **8**

	x	y	z	U_{eq}
Co(11)	7788(1)	733(1)	8679(1)	25(1)
Co(12)	8133(1)	−742(1)	9189(1)	25(1)
C(11)	7602(2)	520(4)	9305(2)	27(1)
C(12)	7301(2)	−212(4)	9063(2)	27(2)
C(13)	6707(2)	−725(4)	9057(2)	27(1)
C(14)	6261(2)	−371(5)	9360(2)	37(2)
C(15)	5699(2)	−910(5)	9348(2)	45(2)
C(16)	5585(2)	−1715(5)	9047(2)	40(2)
C(17)	6046(3)	−2001(5)	8777(2)	39(2)
Br(1)	5930(1)	−3133(1)	8357(1)	79(1)
N(1)	6599(2)	−1548(4)	8771(1)	32(1)
C(110)	7565(2)	1342(4)	9656(2)	25(1)
C(111)	8027(2)	1624(4)	9956(2)	29(1)
C(112)	7812(2)	2490(4)	10226(2)	35(2)
C(113)	7217(2)	2763(4)	10083(2)	37(2)
C(114)	7060(2)	2064(4)	9737(2)	28(1)
Fe(1)	7253(1)	1152(1)	10283(1)	31(1)
C(115)	6929(3)	−430(5)	10369(2)	47(2)
C(116)	7438(3)	−245(5)	10635(2)	48(2)
C(117)	7305(3)	640(6)	10913(2)	50(2)
C(118)	6718(3)	1027(6)	10822(2)	50(2)
C(119)	6481(3)	361(5)	10482(2)	45(2)
P(11)	7840(1)	−227(1)	8055(1)	26(1)
C(120)	8490(2)	112(4)	7703(2)	25(2)
C(121)	8859(2)	−685(5)	7519(2)	37(2)
C(122)	9333(3)	−362(6)	7255(2)	41(2)
C(123)	9442(2)	727(6)	7182(2)	46(2)
C(124)	9086(2)	1540(5)	7373(2)	45(2)
C(125)	8616(2)	1211(5)	7632(2)	34(1)
C(130)	7212(2)	−270(4)	7655(2)	26(1)
C(131)	7314(2)	−475(4)	7220(2)	30(1)
C(132)	6833(2)	−610(4)	6936(2)	34(2)
C(133)	6249(3)	−529(5)	7084(2)	40(2)
C(134)	6143(3)	−334(5)	7518(2)	47(2)
C(135)	6622(3)	−178(5)	7802(2)	34(2)
C(136)	7888(2)	−1692(4)	8181(2)	24(1)
P(12)	8350(1)	−1955(1)	8666(1)	24(1)
C(140)	9118(2)	−1978(4)	8448(2)	22(1)
C(141)	9521(2)	−1128(4)	8521(2)	33(1)
C(142)	10083(3)	−1131(5)	8346(2)	45(2)
C(143)	10281(3)	−1968(5)	8074(2)	49(2)
C(144)	9882(3)	−2827(5)	7986(2)	44(2)
C(145)	9309(2)	−2832(4)	8164(2)	34(1)
C(150)	8192(2)	−3408(4)	8786(2)	23(1)
C(151)	7616(2)	−3851(4)	8718(2)	35(1)
C(152)	7478(3)	−4926(4)	8830(2)	38(2)
C(153)	7896(3)	−5585(5)	9031(2)	45(2)
C(154)	8460(3)	−5151(5)	9103(2)	45(2)
C(155)	8610(2)	−4088(5)	8981(2)	37(2)
C(161)	7259(2)	1740(5)	8523(2)	34(1)
O(161)	6902(2)	2384(3)	8414(2)	63(1)
C(162)	8476(3)	1535(4)	8693(2)	32(1)
O(162)	8919(2)	2013(3)	8731(1)	57(1)
C(171)	7954(3)	−1732(5)	9593(2)	39(2)
O(171)	7841(2)	−2360(4)	9860(2)	70(2)
C(172)	8834(3)	−213(5)	9397(2)	31(2)
O(172)	9256(2)	155(4)	9554(2)	53(1)
Co(21)	9740(1)	−4104(1)	11162(1)	24(1)
Co(22)	9434(1)	−5649(1)	10678(1)	23(1)
C(21)	9945(2)	−4395(4)	10547(2)	24(1)
C(22)	10245(2)	−5091(4)	10809(2)	20(1)
C(23)	10860(2)	−5598(4)	10819(2)	25(1)
C(24)	11293(2)	−5297(5)	10522(2)	33(2)
C(25)	11848(2)	−5802(5)	10517(2)	46(2)
C(26)	11985(2)	−6573(5)	10830(2)	43(2)
C(27)	11531(2)	−6803(4)	11122(2)	36(2)
Br(2)	11685(1)	−7847(1)	11571(1)	76(1)
N(2)	10981(2)	−6346(3)	11130(1)	31(1)
C(210)	10005(2)	−3596(4)	10197(2)	22(1)
C(211)	10507(2)	−2848(4)	10117(2)	32(1)
C(212)	10346(2)	−2172(5)	9759(2)	39(2)
C(213)	9769(2)	−2481(4)	9609(2)	36(1)
C(214)	9557(2)	−3347(5)	9883(2)	33(2)
Fe(2)	10340(1)	−3802(1)	9577(1)	33(1)
C(215)	10683(3)	−5382(5)	9506(2)	43(2)
C(216)	11125(3)	−4587(5)	9395(2)	47(2)
C(217)	10903(3)	−3945(5)	9050(2)	55(2)
C(218)	10314(3)	−4374(7)	8940(2)	60(2)
C(219)	10183(3)	−5220(6)	9224(2)	48(2)
P(21)	9647(1)	−4967(1)	11799(1)	24(1)
C(220)	8964(2)	−4754(4)	12125(2)	23(1)
C(221)	8660(2)	−3752(5)	12102(2)	40(2)
C(222)	8150(2)	−3548(5)	12344(2)	40(2)
C(223)	7921(2)	−4337(5)	12618(2)	36(2)
C(224)	8207(2)	−5324(5)	12653(2)	37(2)
C(225)	8734(2)	−5530(5)	12401(2)	34(1)
C(230)	10244(2)	−4745(4)	12207(2)	26(1)
C(231)	10150(2)	−4276(5)	12611(2)	40(2)
C(232)	10619(3)	−4108(5)	12904(2)	49(2)
C(233)	11196(3)	−4426(5)	12797(2)	40(2)
C(234)	11319(3)	−4883(5)	12403(2)	39(2)
C(235)	10842(3)	−5041(4)	12104(2)	39(2)
C(236)	9690(2)	−6453(4)	11702(2)	26(1)
P(22)	9235(1)	−6801(1)	11221(1)	23(1)
C(240)	8454(2)	−6863(4)	11447(2)	24(1)
C(241)	8039(2)	−6048(4)	11339(2)	33(1)
C(242)	7448(2)	−6083(5)	11520(2)	44(2)
C(243)	7301(2)	−6905(5)	11799(2)	40(2)
C(244)	7714(3)	−7704(5)	11916(2)	43(2)
C(245)	8295(2)	−7692(4)	11735(2)	38(2)
C(250)	9422(2)	−8240(4)	11122(2)	25(1)
C(251)	9009(2)	−8924(4)	10897(2)	33(1)
C(252)	9177(3)	−9981(5)	10769(2)	45(2)
C(253)	9745(3)	−10373(5)	10863(2)	40(2)
C(254)	10148(3)	−9731(5)	11085(2)	39(2)
C(255)	9992(2)	−8678(4)	11207(2)	32(1)
C(261)	10301(3)	−3145(4)	11313(2)	33(1)
O(261)	10683(2)	−2551(3)	11394(1)	52(1)
C(262)	9078(3)	−3263(5)	11080(2)	32(2)
O(262)	8661(2)	−2724(3)	11003(1)	57(1)
C(271)	9623(3)	−6658(5)	10287(2)	40(2)
O(271)	9743(2)	−7319(4)	10032(2)	70(2)
C(272)	8732(3)	−5156(5)	10458(2)	32(2)
O(272)	8310(2)	−4812(3)	10296(2)	53(1)

U_{eq} is defined as one third of the trace of the orthogonalised U_{ij} tensor.

band gave **13** as a dark brown solid (0.2 g, 65%). Calc. for $C_{27}H_{21}Co_4NO_{12}Si_2$: C, 38.43; H, 2.49; N, 1.66. Found: C, 39.04; H, 2.61; N, 1.72%. EIMS (m/z): [MH^+] 844, [$MH^+ - CO$] 816, [$MH^+ - 2CO$] 787. ^{1}H-NMR ($CDCl_3$): δ, 0.39 (s, 18H, $-CH_3$), 7.35 (d, 2H,

Table 5
Anisotropic displacement parameters ($Å^2 \times 10^3$) for **8**

	U^{11}	U^{22}	U^{33}	U^{23}	U^{13}	U^{12}
Co(11)	24(1)	25(1)	25(1)	−1(1)	3(1)	−1(1)
Co(12)	22(1)	27(1)	24(1)	−3(1)	0(1)	1(1)
C(11)	21(3)	30(4)	30(4)	−3(3)	4(3)	5(3)
C(12)	18(3)	30(3)	32(5)	−6(3)	1(3)	−2(3)
C(13)	25(3)	31(3)	25(3)	5(3)	0(2)	−2(3)
C(14)	16(3)	38(4)	55(5)	−11(3)	5(3)	0(3)
C(15)	28(3)	48(4)	57(5)	−8(4)	11(3)	0(3)
C(16)	23(3)	46(4)	52(4)	−9(3)	0(3)	−11(3)
C(17)	33(3)	49(4)	35(4)	−5(3)	−3(3)	−11(3)
Br(1)	64(1)	103(1)	69(1)	−46(1)	14(1)	−45(1)
N(1)	28(3)	36(3)	32(3)	−6(2)	−5(2)	−11(2)
C(110)	19(3)	25(3)	32(4)	−1(3)	6(3)	−2(2)
C(111)	28(3)	36(4)	23(3)	−4(3)	2(3)	−5(3)
C(112)	31(3)	32(3)	41(4)	−18(3)	12(3)	−9(3)
C(113)	31(3)	26(3)	53(4)	−11(3)	10(3)	4(3)
C(114)	26(3)	24(3)	35(4)	−1(3)	2(3)	0(2)
Fe(1)	29(1)	36(1)	27(1)	−6(1)	5(1)	2(1)
C(115)	50(4)	47(4)	42(5)	4(4)	13(4)	−18(4)
C(116)	48(4)	47(4)	50(5)	5(4)	16(4)	19(3)
C(117)	52(4)	78(5)	21(4)	1(4)	3(3)	−19(4)
C(118)	49(4)	67(5)	34(4)	−4(4)	18(3)	1(4)
C(119)	39(4)	58(4)	39(5)	6(4)	12(3)	−(4)
P(11)	22(1)	30(1)	25(1)	−2(1)	2(1)	−1(1)
C(120)	18(3)	33(4)	25(4)	3(3)	4(3)	−1(2)
C(121)	27(3)	36(4)	46(4)	5(3)	20(3)	9(3)
C(122)	34(4)	57(5)	32(4)	11(4)	6(3)	20(3)
C(123)	28(3)	75(5)	35(4)	11(4)	9(3)	−3(3)
C(124)	46(4)	48(4)	42(4)	0(3)	10(3)	−13(3)
C(125)	31(3)	39(4)	31(3)	−3(3)	13(3)	−8(3)
C(130)	28(3)	21(3)	28(4)	6(3)	1(3)	0(3)
C(131)	29(3)	36(4)	27(4)	−11(3)	3(3)	1(3)
C(132)	39(3)	42(4)	23(3)	−7(3)	−2(3)	2(3)
C(133)	42(4)	37(4)	41(4)	3(3)	−9(3)	−7(3)
C(134)	30(4)	71(5)	39(5)	1(4)	−3(3)	11(3)
C(135)	28(3)	58(4)	17(4)	−4(3)	6(3)	2(3)
C(136)	22(3)	32(3)	19(3)	−5(2)	5(2)	−3(2)
P(12)	21(1)	27(1)	22(1)	−2(1)	1(1)	0(1)
C(140)	27(3)	21(3)	19(3)	2(2)	1(2)	7(2)
C(141)	30(3)	32(3)	37(4)	−6(3)	7(3)	−6(3)
C(142)	39(4)	48(4)	47(4)	−10(4)	4(3)	−18(3)
C(143)	30(3)	62(5)	56(5)	14(4)	8(3)	0(3)
C(144)	41(4)	47(4)	44(4)	−8(3)	24(3)	1(3)
C(145)	38(3)	35(4)	28(3)	−4(3)	0(3)	6(3)
C(150)	28(3)	24(3)	18(3)	0(2)	1(2)	−5(2)
C(151)	27(3)	35(3)	42(4)	7(3)	−1(3)	−5(2)
C(152)	31(4)	33(4)	50(5)	3(3)	−5(3)	−16(3)
C(153)	58(4)	28(4)	49(4)	6(3)	10(3)	−14(3)
C(154)	42(4)	36(4)	58(6)	20(3)	−6(3)	−1(3)
C(155)	32(3)	37(4)	42(4)	6(3)	2(3)	−9(3)
C(161)	29(3)	38(4)	34(4)	−1(3)	8(3)	−2(3)
O(161)	57(3)	58(3)	75(3)	4(3)	−4(3)	28(2)
C(162)	41(4)	35(4)	20(3)	−8(3)	3(3)	0(3)
O(162)	36(2)	63(3)	72(3)	7(3)	−6(2)	−27(2)
C(171)	45(4)	43(4)	29(4)	−6(3)	−2(3)	15(3)
O(171)	95(4)	64(3)	51(4)	30(3)	23(3)	20(3)
C(172)	21(3)	37(4)	35(5)	−5(3)	6(3)	13(3)
O(172)	22(2)	72(3)	66(4)	−30(3)	−5(3)	1(2)
Co(21)	22(1)	26(1)	25(1)	1(1)	1(1)	2(1)
Co(22)	19(1)	26(1)	23(1)	3(1)	0(1)	−1(1)
C(21)	18(3)	29(3)	27(3)	−4(3)	−3(2)	4(3)
C(22)	17(3)	25(3)	19(4)	2(2)	4(3)	−3(2)
C(23)	23(3)	31(3)	21(3)	0(3)	−1(2)	5(3)

Table 5 (*Continued*)

	U^{11}	U^{22}	U^{33}	U^{23}	U^{13}	U^{12}
C(24)	24(3)	37(4)	38(4)	13(3)	8(3)	6(3)
C(25)	30(3)	49(4)	58(5)	10(4)	17(3)	4(3)
C(26)	23(3)	52(4)	54(5)	−1(4)	0(3)	7(3)
C(27)	34(3)	34(3)	42(4)	0(3)	−4(3)	8(3)
Br(2)	60(1)	92(1)	77(1)	45(1)	4(1)	37(1)
N(2)	25(2)	36(3)	30(3)	4(2)	−4(2)	6(2)
C(210)	17(3)	23(3)	26(3)	5(3)	−1(2)	−2(2)
C(211)	32(3)	26(3)	37(4)	6(3)	−2(3)	3(3)
C(212)	36(4)	47(4)	35(4)	13(3)	2(3)	−5(3)
C(213)	42(4)	36(4)	28(4)	3(3)	−3(3)	0(3)
C(214)	23(3)	38(4)	36(4)	7(3)	−3(3)	−5(3)
Fe(2)	31(1)	39(1)	30(1)	5(1)	6(1)	0(1)
C(215)	38(4)	47(4)	42(5)	−2(4)	10(3)	2(3)
C(216)	40(4)	61(5)	41(4)	8(4)	15(3)	11(4)
C(217)	65(5)	56(5)	43(4)	5(4)	27(4)	6(4)
C(218)	50(5)	100(7)	29(4)	1(4)	1(3)	14(4)
C(219)	40(4)	60(5)	43(5)	−16(4)	9(4)	11(3)
P(21)	23(1)	26(1)	22(1)	1(1)	−1(1)	−1(1)
C(220)	24(3)	26(3)	18(4)	8(3)	−8(3)	−4(3)
C(221)	41(3)	48(4)	30(4)	15(3)	9(3)	6(3)
C(222)	35(3)	45(4)	39(4)	−1(3)	5(3)	15(3)
C(223)	19(3)	52(4)	37(4)	−7(3)	5(3)	−4(3)
C(224)	32(3)	41(4)	38(4)	1(3)	9(3)	0(3)
C(225)	38(3)	32(4)	32(4)	−3(3)	−5(3)	11(3)
C(230)	26(3)	28(3)	23(4)	6(3)	4(3)	−5(3)
C(231)	35(3)	44(4)	41(4)	−11(3)	3(3)	−5(3)
C(232)	55(4)	51(4)	41(4)	−11(3)	−8(3)	−15(3)
C(233)	33(4)	50(4)	38(4)	1(3)	−16(3)	−5(3)
C(234)	30(3)	51(4)	36(5)	10(3)	−8(3)	−9(3)
C(235)	39(4)	52(4)	25(4)	−1(3)	−3(3)	−1(3)
C(236)	18(3)	36(3)	25(3)	1(3)	−3(2)	4(2)
P(22)	23(1)	21(1)	26(1)	2(1)	1(1)	1(1)
C(240)	24(3)	29(3)	20(3)	−1(3)	3(2)	−2(2)
C(241)	28(3)	37(4)	34(4)	10(3)	7(3)	9(3)
C(242)	28(3)	53(4)	52(4)	−2(4)	16(3)	8(3)
C(243)	29(3)	46(4)	44(4)	−6(3)	16(3)	2(3)
C(244)	53(4)	27(4)	50(4)	1(3)	22(3)	−11(3)
C(245)	34(3)	34(4)	47(4)	4(3)	13(3)	1(3)
C(250)	29(3)	24(3)	23(3)	3(3)	11(2)	1(2)
C(251)	30(3)	28(4)	41(4)	−3(3)	−4(3)	6(3)
C(252)	45(4)	36(4)	53(5)	−11(3)	−5(3)	10(3)
C(253)	51(4)	26(4)	44(4)	−5(3)	12(3)	12(3)
C(254)	38(4)	39(4)	40(4)	−6(3)	6(3)	14(3)
C(255)	28(3)	33(3)	34(3)	−10(3)	−2(3)	5(2)
C(261)	44(4)	33(4)	21(3)	−1(3)	0(3)	−4(3)
O(261)	55(3)	55(3)	47(3)	−4(2)	−2(2)	−26(2)
C(262)	36(3)	33(4)	27(4)	−3(3)	10(3)	−3(3)
O(262)	49(3)	54(3)	67(3)	4(2)	−7(2)	26(2)
C(271)	43(4)	43(4)	33(4)	2(3)	5(3)	−8(3)
O(271)	96(4)	56(3)	56(4)	−20(3)	33(3)	−21(3)
C(272)	25(3)	36(4)	36(4)	10(3)	3(3)	−5(3)
O(272)	21(2)	75(3)	64(4)	26(3)	−11(2)	−1(2)

The anisotropic displacement factor exponent takes the form: $-2\pi^2[h^2a^{*2}U^{11}+\cdots+2haka^*b^*U^{12}]$.

Ar–H), 7.55 (t, 1H, Ar–H). IR (CH_2Cl_2, cm^{-1}): 2093, 2056, 2021 (ν_{CO}).

4.5.3. Complex **14**

A mixture of **6** (30 mg, 61 μmol) and $Co_2(CO)_8$ (83 mg, 242 μmol) was stirred for 6 h in 30 ml of CH_2Cl_2. The volatiles were removed under reduced pressure to a dark green solid which was separated on silica gel eluent 9:1 CH_2Cl_2–THF to give a dark green powder **14** (30 mg, 47%). Calc. for $C_{41}H_{21}Co_4Fe_2NO_{12}$: C, 46.11; H, 1.96; N, 1.31. Found: C, 46.39; H, 1.92; N, 1.38%. ^{1}H-NMR ($CDCl_3$): δ, 4.07 (s, 10H, $-C_5H_5$), 4.37

(t, 4H, –αC$_5$H$_5$), 4.53 (t, 4H, –βC$_5$H$_5$), 7.60–7.80 (m, 3H, Py–H). IR (CH$_2$Cl$_2$, cm^{-1}): 2091, 2056, 2020 (ν_{CO}).

4.6. Preparation of **18**

Complex **11** (0.1 g, 0.1 mmol) and K$_2$CO$_3$ (76 mg, 0.55 mmol) were stirred at r.t. in MeOH (30 ml) for 72 h. Water (30 ml) was added, and the CH$_2$Cl$_2$ (3 × 50 ml) extracts reduced under reduced pressure to give **18** as a brown–red solid (32 mg, 29%). Calc. for C$_{41}$H$_{35}$Co$_2$NO$_4$P$_2$Si: C, 60.50, H, 4.53; N, 1.72. Found: C, 60.30; H, 4.50; N, 1.78%. EIMS (m/z): [MH$^+$] 814, [M$^+$ − Co] 785. ^{1}H-NMR (CDCl$_3$): δ, 0.46 (s, 9H, –CH$_3$), 3.29 (s, 1H, ≡H), 3.40 (m, 1H, –CH$_2$), 5.16 (m, 1H, –CH$_2$), 7.35 (d, 2H, Ar–H), 7.65 (t, 1H, Ar–H). ^{31}P-NMR (CDCl$_3$): δ, 37.82. IR (CH$_2$Cl$_2$, cm^{-1}): 2020, 1994, 1965 (ν_{CO}), 2055 ($\nu_{C\equiv C}$).

4.7. Preparation of **19**

A mixture of **18** (60 mg, 75 μmol), iodoferrocene (15 mg, 50 μmol), bis(triphenylphosphine)palladium dichloride (5 mg, 7.5 μmol) and copper(I) iodide (2 mg, 10 μmol) in THF (15 ml) and diisopropylamine (25 ml) was refluxed for 8 h under a positive flow of N$_2$. The reaction solution was quenched with water (50 ml), extracted with CH$_2$Cl$_2$ (50 ml), the extracts were dried (MgSO$_4$) and concentrated under reduced pressure. Separation on silica gel, 2:1 C$_6$H$_{14}$–CH$_2$Cl$_2$, gave **19** from the major band (15 mg, 28%). Calc. for C$_{51}$H$_{43}$Co$_2$FeNO$_4$P$_2$Si: C, 62.10; H, 4.22; N, 2.49. Found: C, 62.99; H, 4.99; N, 2.58%. ^{1}H-NMR (CDCl$_3$): δ (ppm) 0.38 (s, 9H, –CH$_3$), 3.19 (q, 2H, –CH$_2$), 4.15 (s, 5H, –C$_5$H$_5$), 4.35 (t, 2H, α-C$_5$H$_5$), 4.51 (t, 2H, β-C$_5$H$_5$), 5.2 (q, 2H, –CH$_2$), 6.80–7.45 (m, 20H, Ar–H). IR (CH$_2$Cl$_2$, cm^{-1}): 2021, 1993, 1964 (ν_{CO}), 2055 ($\nu_{C\equiv C}$).

4.8. Preparation of **20**

Copper(I) chloride (4 mg, 0.04 mmol) and TMEDA (3 g, 4 ml, 0.026 mol) were stirred for 3 h and O$_2$ bubbled into the solution and over a period of 20 min. A solution of **17** (50 mg, 0.0611 mmol) in isopropanol (5 ml) was then added dropwise and the mixture stirred for 2 h, with oxygen bubbling through the reaction mixture. Solvent was removed and the brown solid was separated on silica gel, eluent 2/1 C$_6$H$_{14}$–CH$_2$Cl$_2$ to give **20** as a dark red solid (41%). Calc. for C$_{82}$H$_{68}$Co$_4$N$_2$O$_8$P$_4$Si$_2$: C, 60.62; H, 4.18; N, 1.72. Found: C, 60.76; H, 4.72; N, 1.60%. EIMS (m/z): [MH$^+$] 1625, [(M-monomer unit) H$^+$] 814. ^{1}H-NMR (CDCl$_3$): δ, 0.50 (s, 18H, –CH$_3$), 3.30 (m, 1H, –CH$_2$), 5.20 (m, 1H, –CH$_2$), 7.03–7.51 (m, 46H, Ar–H). ^{31}P-NMR (CDCl$_3$): δ, 37.41. IR (CH$_2$Cl$_2$, cm^{-1}): 2024, 1997, 1971 (ν_{CO}), 2053 ($\nu_{C\equiv C}$).

Table 6
Hydrogen coordinates (× 10^4) and isotropic displacement parameters (Å^2 × 10^3) for **8**

	x	y	z	U_{eq}
H(14)	6340	203	9560	44
H(15)	5392	−717	9550	53
H(16)	5198	−2058	9028	48
H(111)	8416	1289	9974	34
H(112)	8027	2824	10 458	42
H(113)	6966	3323	10 202	44
H(114)	6686	2069	9584	34
H(115)	6892	−983	10 154	56
H(116)	7808	−648	10 628	58
H(117)	7569	928	11 127	60
H(118)	6516	1620	10 961	60
H(119)	6092	434	10 352	54
H(121)	8787	−1442	7574	44
H(122)	9585	−902	7124	49
H(123)	9767	935	6998	55
H(124)	9168	2297	7325	54
H(125)	8369	1753	7766	40
H(131)	7719	−524	7116	37
H(132)	6908	−758	6640	41
H(133)	5918	−606	6890	48
H(134)	5738	−306	7623	56
H(135)	6545	−9	8096	41
H(13A)	8069	−2085	7932	29
H(13B)	7474	−1985	8227	29
H(141)	9400	−528	8698	40
H(142)	10 351	−543	8412	53
H(143)	10 677	−1953	7951	59
H(144)	10 005	−3413	7803	53
H(145)	9037	−3415	8097	40
H(151)	7310	−3405	8591	42
H(152)	7087	−5212	8767	46
H(153)	7799	−6314	9117	54
H(154)	8759	−5591	9241	55
H(155)	9010	−3823	9033	44
H(24)	11 205	−4735	10 318	40
H(25)	12 138	−5624	10 300	55
H(26)	12 370	−6924	10 843	52
H(211)	10 877	−2815	10 275	38
H(212)	10 590	−1602	9641	47
H(213)	9558	−2172	9370	43
H(214)	9174	−3703	9857	39
H(215)	10 715	−5922	9726	51
H(216)	11 509	−4499	9531	56
H(217)	11 105	−3343	8917	66
H(218)	10 060	−4121	8713	72
H(219)	9816	−5628	9230	57
H(221)	8809	−3196	11 915	47
H(222)	7953	−2856	12 321	48
H(223)	7566	−4192	12 782	43
H(224)	8056	−5870	12 844	45
H(225)	8932	−6222	12 425	41
H(231)	9749	−4063	12 690	48
H(232)	10 539	−3775	13 176	59
H(233)	11 516	−4327	13 000	48
H(234)	11 723	−5093	12 331	47
H(235)	10 928	−5353	11 829	46
H(23A)	9533	−6856	11 956	31
H(23B)	10 118	−6673	11 656	31
H(241)	8150	−5474	11 147	40
H(242)	7157	−5536	11 448	53
H(243)	6902	−6931	11 916	48
H(244)	7605	−8256	12 119	52
H(245)	8580	−8249	11 808	46
H(251)	8614	−8660	10 831	40
H(252)	8897	−10 429	10 615	54
H(253)	9859	−11 092	10 775	48
H(254)	10 539	−10 012	11 155	47
H(255)	10 284	−8239	11 353	38

Table 7
Bond lengths (Å) and angles (°) for **8**

Bond lengths			
Co(11)–C(161)	1.758(6)	Co(21)–C(261)	1.762(6)
Co(11)–C(162)	1.801(6)	Co(21)–C(262)	1.797(6)
Co(11)–C(12)	1.969(6)	Co(21)–C(22)	1.967(5)
Co(11)–C(11)	1.994(5)	Co(21)–C(21)	1.989(5)
Co(11)–P(11)	2.2612(19)	Co(21)–P(21)	2.2433(19)
Co(11)–Co(12)	2.5059(11)	Co(21)–Co(22)	2.4956(11)
Co(12)–C(171)	1.780(7)	Co(22)–C(271)	1.772(7)
Co(12)–C(172)	1.790(7)	Co(22)–C(272)	1.791(6)
Co(12)–C(11)	1.961(5)	Co(22)–C(21)	1.937(5)
Co(12)–C(12)	1.979(5)	Co(22)–C(22)	1.953(5)
Co(12)–P(12)	2.2416(17)	Co(22)–P(22)	2.2311(17)
C(11)–C(12)	1.338(7)	C(21)–C(22)	1.347(7)
C(11)–C(110)	1.479(7)	C(21)–C(210)	1.460(7)
C(12)–C(13)	1.450(7)	C(22)–C(23)	1.488(7)
C(13)–N(1)	1.359(6)	C(23)–N(2)	1.351(6)
C(13)–C(14)	1.423(7)	C(23)–C(24)	1.375(7)
C(14)–C(15)	1.400(7)	C(24)–C(25)	1.368(7)
C(15)–C(16)	1.374(7)	C(25)–C(26)	1.381(7)
C(16)–C(17)	1.359(7)	C(26)–C(27)	1.377(7)
C(17)–N(1)	1.335(6)	C(27)–N(2)	1.332(6)
C(17)–Br(1)	1.910(6)	C(27)–Br(2)	1.911(6)
C(110)–C(111)	1.419(7)	C(210)–C(214)	1.420(7)
C(110)–C(114)	1.438(6)	C(210)–C(211)	1.452(6)
C(110)–Fe(1)	2.071(5)	C(210)–Fe(2)	2.071(5)
C(111)–C(112)	1.425(7)	C(211)–C(212)	1.423(7)
C(111)–Fe(1)	2.062(5)	C(211)–Fe(2)	2.066(5)
C(112)–C(113)	1.421(7)	C(212)–C(213)	1.404(7)
C(112)–Fe(1)	2.048(5)	C(212)–Fe(2)	2.060(6)
C(113)–C(114)	1.411(7)	C(213)–C(214)	1.430(7)
C(113)–Fe(1)	2.056(5)	C(213)–Fe(2)	2.041(5)
C(114)–Fe(1)	2.064(5)	C(214)–Fe(2)	2.041(5)
Fe(1)–C(119)	2.047(6)	Fe(2)–C(219)	2.070(7)
Fe(1)–C(116)	2.059(6)	Fe(2)–C(216)	2.053(6)
Fe(1)–C(117)	2.052(6)	Fe(2)–C(217)	2.056(6)
Fe(1)–C(118)	2.050(6)	Fe(2)–C(215)	2.076(6)
Fe(1)–C(115)	2.068(6)	Fe(2)–C(218)	2.091(7)
C(115)–C(116)	1.408(9)	C(215)–C(216)	1.414(8)
C(115)–C(119)	1.420(8)	C(215)–C(219)	1.416(8)
C(116)–C(117)	1.409(8)	C(216)–C(217)	1.408(8)
C(117)–C(118)	1.403(8)	C(217)–C(218)	1.438(8)
C(118)–C(119)	1.428(8)	C(218)–C(219)	1.383(9)
P(11)–C(136)	1.826(5)	P(21)–C(220)	1.828(6)
P(11)–C(120)	1.845(6)	P(21)–C(236)	1.833(5)
P(11)–C(130)	1.855(6)	P(21)–C(230)	1.842(6)
C(120)–C(125)	1.382(7)	C(220)–C(225)	1.370(7)
C(120)–C(121)	1.385(7)	C(220)–C(221)	1.392(7)
C(121)–C(122)	1.382(7)	C(221)–C(222)	1.370(7)
C(122)–C(123)	1.365(8)	C(222)–C(223)	1.376(7)
C(123)–C(124)	1.391(8)	C(223)–C(224)	1.359(7)
C(124)–C(125)	1.368(7)	C(224)–C(225)	1.419(7)
C(130)–C(135)	1.380(7)	C(230)–C(231)	1.390(8)
C(130)–C(131)	1.387(8)	C(230)–C(235)	1.402(8)
C(131)–C(132)	1.386(7)	C(231)–C(232)	1.389(7)
C(132)–C(133)	1.367(7)	C(232)–C(233)	1.369(8)
C(133)–C(134)	1.386(8)	C(233)–C(234)	1.369(8)
C(134)–C(135)	1.384(8)	C(234)–C(235)	1.413(8)
C(136)–P(12)	1.842(5)	C(236)–P(22)	1.842(5)
P(12)–C(140)	1.820(5)	P(22)–C(250)	1.824(5)
P(12)–C(150)	1.838(5)	P(22)–C(240)	1.858(5)
C(140)–C(141)	1.381(6)	C(240)–C(241)	1.387(6)
C(140)–C(145)	1.423(6)	C(240)–C(245)	1.391(7)
C(141)–C(142)	1.349(7)	C(241)–C(242)	1.417(6)
C(142)–C(143)	1.392(7)	C(242)–C(243)	1.359(7)

Table 7 (*Continued*)

C(143)–C(144)	1.392(7)	C(243)–C(244)	1.380(7)
C(144)–C(145)	1.376(7)	C(244)–C(245)	1.396(7)
C(150)–C(155)	1.376(7)	C(250)–C(255)	1.387(6)
C(150)–C(151)	1.394(6)	C(250)–C(251)	1.416(7)
C(151)–C(152)	1.386(7)	C(251)–C(252)	1.393(7)
C(152)–C(153)	1.369(8)	C(252)–C(253)	1.369(8)
C(153)–C(154)	1.367(8)	C(253)–C(254)	1.366(8)
C(154)–C(155)	1.386(7)	C(254)–C(255)	1.377(7)
C(161)–O(161)	1.159(6)	C(261)–O(261)	1.137(5)
C(162)–O(162)	1.141(6)	C(262)–O(262)	1.153(6)
C(171)–O(171)	1.152(7)	C(271)–O(271)	1.158(7)
C(172)–O(172)	1.140(6)	C(272)–O(272)	1.136(6)
Bond angles			
C(161)–Co(11)–C(162)	100.7(2)	C(11)–C(12)–C(13)	137.7(6)
C(161)–Co(11)–C(12)	102.3(2)	C(11)–C(12)–Co(11)	71.3(3)
C(162)–Co(11)–C(12)	139.4(3)	C(13)–C(12)–Co(11)	137.3(5)
C(161)–Co(11)–C(11)	102.9(2)	C(11)–C(12)–Co(12)	69.4(3)
C(162)–Co(11)–C(11)	102.7(2)	C(13)–C(12)–Co(12)	134.2(4)
C(12)–Co(11)–C(11)	39.4(2)	Co(11)–C(12)–Co(12)	78.8(2)
C(161)–Co(11)–P(11)	99.01(18)	N(1)–C(13)–C(14)	122.2(5)
C(162)–Co(11)–P(11)	104.83(18)	N(1)–C(13)–C(12)	118.8(5)
C(12)–Co(11)–P(11)	104.01(18)	C(14)–C(13)–C(12)	119.0(5)
C(11)–Co(11)–P(11)	140.62(16)	C(15)–C(14)–C(13)	116.7(5)
C(161)–Co(11)–Co(12)	150.79(18)	C(16)–C(15)–C(14)	120.9(5)
C(162)–Co(11)–Co(12)	96.78(18)	C(17)–C(16)–C(15)	117.5(5)
C(12)–Co(11)–Co(12)	50.79(16)	N(1)–C(17)–C(16)	125.8(5)
C(11)–Co(11)–Co(12)	50.10(14)	N(1)–C(17)–Br(1)	114.1(4)
P(11)–Co(11)–Co(12)	98.84(5)	C(16)–C(17)–Br(1)	120.1(4)
C(171)–Co(12)–C(172)	100.4(3)	C(17)–N(1)–C(13)	116.9(5)
C(171)–Co(12)–C(11)	105.6(2)	C(111)–C(110)–C(114)	106.9(5)
C(172)–Co(12)–C(11)	99.6(2)	C(111)–C(110)–C(11)	127.2(5)
C(171)–Co(12)–C(12)	98.9(3)	C(114)–C(110)–C(11)	125.7(5)
C(172)–Co(12)–C(12)	138.6(2)	C(111)–C(110)–Fe(1)	69.6(3)
C(11)–Co(12)–C(12)	39.7(2)	C(114)–C(110)–Fe(1)	69.4(3)
C(171)–Co(12)–P(12)	96.3(2)	C(11)–C(110)–Fe(1)	129.1(4)
C(172)–Co(12)–P(12)	108.19(18)	C(110)–C(111)–C(112)	109.0(5)
C(11)–Co(12)–P(12)	140.66(17)	C(110)–C(111)–Fe(1)	70.3(3)
C(12)–Co(12)–P(12)	105.59(18)	C(112)–C(111)–Fe(1)	69.2(3)
C(171)–Co(12)–Co(11)	149.24(18)	C(113)–C(112)–C(111)	107.2(5)
C(172)–Co(12)–Co(11)	103.3(2)	C(113)–C(112)–Fe(1)	70.0(3)
C(11)–Co(12)–Co(11)	51.28(16)	C(111)–C(112)–Fe(1)	70.2(3)
C(12)–Co(12)–Co(11)	50.42(18)	C(114)–C(113)–C(112)	108.7(5)
P(12)–Co(12)–Co(11)	94.64(5)	C(114)–C(113)–Fe(1)	70.3(3)
C(12)–C(11)–C(110)	146.4(5)	C(112)–C(113)–Fe(1)	69.5(3)
C(12)–C(11)–Co(12)	70.9(3)	C(113)–C(114)–C(110)	108.2(5)
C(110)–C(11)–Co(12)	134.1(4)	C(113)–C(114)–Fe(1)	69.7(3)
C(12)–C(11)–Co(11)	69.2(4)	C(110)–C(114)–Fe(1)	69.9(3)
C(110)–C(11)–Co(11)	129.5(4)	C(119)–Fe(1)–C(112)	153.9(2)
Co(12)–C(11)–Co(11)	78.62(19)	C(119)–Fe(1)–C(116)	67.5(3)
C(112)–Fe(1)–C(116)	125.6(3)	C(117)–Fe(1)–C(110)	155.1(2)
C(119)–Fe(1)–C(117)	67.5(3)	C(118)–Fe(1)–C(110)	164.2(2)
C(112)–Fe(1)–C(117)	106.8(3)	C(113)–Fe(1)–C(110)	68.0(2)
C(116)–Fe(1)–C(117)	40.1(2)	C(115)–Fe(1)–C(110)	109.9(2)
C(119)–Fe(1)–C(118)	40.8(2)	C(111)–Fe(1)–C(110)	40.16(19)
C(112)–Fe(1)–C(118)	118.3(2)	C(114)–Fe(1)–C(110)	40.70(18)
C(116)–Fe(1)–C(118)	67.7(3)	C(116)–C(115)–C(119)	107.5(6)
C(117)–Fe(1)–C(118)	40.0(2)	C(116)–C(115)–Fe(1)	69.7(4)
C(119)–Fe(1)–C(113)	120.4(2)	C(119)–C(115)–Fe(1)	69.0(4)
C(112)–Fe(1)–C(113)	40.52(19)	C(115)–C(116)–C(117)	108.2(6)
C(116)–Fe(1)–C(113)	162.3(3)	C(115)–C(116)–Fe(1)	70.4(4)
C(117)–Fe(1)–C(113)	125.2(3)	C(117)–C(116)–Fe(1)	69.7(4)
C(118)–Fe(1)–C(113)	107.0(2)	C(118)–C(117)–C(116)	109.0(6)
C(119)–Fe(1)–C(115)	40.4(2)	C(118)–C(117)–Fe(1)	69.9(4)
C(112)–Fe(1)–C(115)	163.2(2)	C(116)–C(117)–Fe(1)	70.2(4)
C(116)–Fe(1)–C(115)	39.9(2)	C(117)–C(118)–C(119)	107.1(6)

Table 7 (*Continued*)

C(117)–Fe(1)–C(115)	67.3(3)	C(117)–C(118)–Fe(1)	70.1(3)
C(118)–Fe(1)–C(115)	68.1(3)	C(119)–C(118)–Fe(1)	69.5(3)
C(113)–Fe(1)–C(115)	155.7(2)	C(115)–C(119)–C(118)	108.2(6)
C(119)–Fe(1)–C(111)	164.5(2)	C(115)–C(119)–Fe(1)	70.6(4)
C(112)–Fe(1)–C(111)	40.56(19)	C(118)–C(119)–Fe(1)	69.7(3)
C(116)–Fe(1)–C(111)	109.0(2)	C(136)–P(11)–C(120)	107.4(2)
C(117)–Fe(1)–C(111)	120.3(2)	C(136)–P(11)–C(130)	99.1(2)
C(118)–Fe(1)–C(111)	153.5(2)	C(120)–P(11)–C(130)	101.0(3)
C(113)–Fe(1)–C(111)	67.6(2)	C(136)–P(11)–Co(11)	108.88(17)
C(115)–Fe(1)–C(111)	127.4(2)	C(120)–P(11)–Co(11)	115.4(2)
C(119)–Fe(1)–C(114)	109.2(2)	C(130)–P(11)–Co(11)	123.15(19)
C(112)–Fe(1)–C(114)	68.0(2)	C(125)–C(120)–C(121)	119.5(5)
C(116)–Fe(1)–C(114)	156.5(3)	C(125)–C(120)–P(11)	117.7(4)
C(117)–Fe(1)–C(114)	162.2(2)	C(121)–C(120)–P(11)	122.7(4)
C(118)–Fe(1)–C(114)	126.0(2)	C(122)–C(121)–C(120)	119.1(6)
C(113)–Fe(1)–C(114)	40.1(2)	C(123)–C(122)–C(121)	120.3(6)
C(115)–Fe(1)–C(114)	122.3(2)	C(122)–C(123)–C(124)	121.4(6)
C(111)–Fe(1)–C(114)	67.6(2)	C(125)–C(124)–C(123)	117.8(6)
C(119)–Fe(1)–C(110)	127.6(2)	C(124)–C(125)–C(120)	121.8(5)
C(112)–Fe(1)–C(110)	68.4(2)	C(135)–C(130)–C(131)	119.0(5)
C(116)–Fe(1)–C(110)	121.5(2)	C(135)–C(130)–P(11)	118.6(5)
C(131)–C(130)–P(11)	122.1(4)	C(262)–Co(21)–C(21)	98.6(2)
C(132)–C(131)–C(130)	121.0(5)	C(22)–Co(21)–C(21)	39.8(2)
C(133)–C(132)–C(131)	119.8(5)	C(261)–Co(21)–P(21)	98.06(18)
C(132)–C(133)–C(134)	119.7(6)	C(262)–Co(21)–P(21)	108.45(18)
C(135)–C(134)–C(133)	120.7(6)	C(22)–Co(21)–P(21)	104.70(18)
C(134)–C(135)–C(130)	119.8(6)	C(21)–Co(21)–P(21)	141.17(17)
P(11)–C(136)–P(12)	112.1(3)	C(261)–Co(21)–Co(22)	147.83(17)
C(140)–P(12)–C(136)	102.2(2)	C(262)–Co(21)–Co(22)	97.21(18)
C(140)–P(12)–C(150)	103.7(2)	C(22)–Co(21)–Co(22)	50.19(16)
C(136)–P(12)–C(150)	103.2(2)	C(21)–Co(21)–Co(22)	49.62(15)
C(140)–P(12)–Co(12)	118.42(17)	P(21)–Co(21)–Co(22)	98.69(5)
C(136)–P(12)–Co(12)	110.91(16)	C(271)–Co(22)–C(272)	100.1(3)
C(150)–P(12)–Co(12)	116.49(17)	C(271)–Co(22)–C(21)	105.4(2)
C(141)–C(140)–C(145)	117.2(5)	C(272)–Co(22)–C(21)	99.1(2)
C(141)–C(140)–P(12)	121.6(4)	C(271)–Co(22)–C(22)	99.7(2)
C(145)–C(140)–P(12)	121.0(4)	C(272)–Co(22)–C(22)	138.7(2)
C(142)–C(141)–C(140)	121.4(5)	C(21)–Co(22)–C(22)	40.5(2)
C(141)–C(142)–C(143)	122.2(5)	C(271)–Co(22)–P(22)	97.2(2)
C(144)–C(143)–C(142)	117.9(5)	C(272)–Co(22)–P(22)	109.09(19)
C(145)–C(144)–C(143)	120.3(6)	C(21)–Co(22)–P(22)	139.95(16)
C(144)–C(145)–C(140)	121.0(5)	C(22)–Co(22)–P(22)	103.90(18)
C(155)–C(150)–C(151)	116.3(5)	C(271)–Co(22)–Co(21)	150.21(19)
C(155)–C(150)–P(12)	122.6(4)	C(272)–Co(22)–Co(21)	102.0(2)
C(151)–C(150)–P(12)	120.8(4)	C(21)–Co(22)–Co(21)	51.45(15)
C(152)–C(151)–C(150)	121.7(5)	C(22)–Co(22)–Co(21)	50.72(16)
C(153)–C(152)–C(151)	121.2(6)	P(22)–Co(22)–Co(21)	94.16(5)
C(154)–C(153)–C(152)	117.3(6)	C(22)–C(21)–C(210)	145.1(5)
C(153)–C(154)–C(155)	122.1(6)	C(22)–C(21)–Co(22)	70.4(3)
C(150)–C(155)–C(154)	121.3(5)	C(210)–C(21)–Co(22)	137.1(4)
O(161)–C(161)–Co(11)	178.3(5)	C(22)–C(21)–Co(21)	69.2(3)
O(162)–C(162)–Co(11)	175.0(5)	C(210)–C(21)–Co(21)	127.7(4)
O(171)–C(171)–Co(12)	178.9(6)	Co(22)–C(21)–Co(21)	78.9(2)
O(172)–C(172)–Co(12)	174.9(5)	C(21)–C(22)–C(23)	136.0(5)
C(261)–Co(21)–C(262)	103.2(2)	C(21)–C(22)–Co(22)	69.1(3)
C(261)–Co(21)–C(22)	98.9(2)	C(23)–C(22)–Co(22)	133.8(4)
C(262)–Co(21)–C(22)	136.7(3)	C(21)–C(22)–Co(21)	71.0(3)
C(261)–Co(21)–C(21)	102.3(2)	C(23)–C(22)–Co(21)	139.1(4)
Co(22)–C(22)–Co(21)	79.09(19)	C(216)–Fe(2)–C(212)	121.1(2)
N(2)–C(23)–C(24)	121.4(4)	C(217)–Fe(2)–C(212)	107.1(2)
N(2)–C(23)–C(22)	118.2(5)	C(214)–Fe(2)–C(210)	40.39(18)
C(24)–C(23)–C(22)	120.4(5)	C(213)–Fe(2)–C(210)	69.0(2)
C(25)–C(24)–C(23)	120.4(5)	C(216)–Fe(2)–C(210)	127.6(2)
C(24)–C(25)–C(26)	119.5(5)	C(217)–Fe(2)–C(210)	163.7(2)
C(27)–C(26)–C(25)	116.1(5)	C(212)–Fe(2)–C(210)	68.5(2)

Table 7 (*Continued*)

N(2)–C(27)–C(26)	126.0(5)	C(214)–Fe(2)–C(211)	67.9(2)
N(2)–C(27)–Br(2)	115.0(4)	C(213)–Fe(2)–C(211)	68.3(2)
C(26)–C(27)–Br(2)	119.0(4)	C(216)–Fe(2)–C(211)	109.5(2)
C(27)–N(2)–C(23)	116.5(5)	C(217)–Fe(2)–C(211)	125.5(2)
C(214)–C(210)–C(211)	106.1(5)	C(212)–Fe(2)–C(211)	40.35(19)
C(214)–C(210)–C(21)	125.9(4)	C(210)–Fe(2)–C(211)	41.10(18)
C(211)–C(210)–C(21)	127.9(4)	C(214)–Fe(2)–C(215)	127.4(2)
C(214)–C(210)–Fe(2)	68.7(3)	C(213)–Fe(2)–C(215)	163.1(2)
C(211)–C(210)–Fe(2)	69.3(3)	C(216)–Fe(2)–C(215)	40.0(2)
C(21)–C(210)–Fe(2)	129.8(3)	C(217)–Fe(2)–C(215)	67.5(3)
C(212)–C(211)–C(210)	107.8(5)	C(212)–Fe(2)–C(215)	156.5(2)
C(212)–C(211)–Fe(2)	69.6(3)	C(210)–Fe(2)–C(215)	109.9(2)
C(210)–C(211)–Fe(2)	69.6(3)	C(211)–Fe(2)–C(215)	122.7(2)
C(213)–C(212)–C(211)	109.2(5)	C(214)–Fe(2)–C(219)	109.2(2)
C(213)–C(212)–Fe(2)	69.3(3)	C(213)–Fe(2)–C(219)	125.3(2)
C(211)–C(212)–Fe(2)	70.1(3)	C(216)–Fe(2)–C(219)	66.9(3)
C(212)–C(213)–C(214)	107.2(5)	C(217)–Fe(2)–C(219)	67.1(3)
C(212)–C(213)–Fe(2)	70.7(3)	C(212)–Fe(2)–C(219)	161.2(3)
C(214)–C(213)–Fe(2)	69.5(3)	C(210)–Fe(2)–C(219)	122.1(3)
C(210)–C(214)–C(213)	109.7(5)	C(211)–Fe(2)–C(219)	157.5(3)
C(210)–C(214)–Fe(2)	70.9(3)	C(215)–Fe(2)–C(219)	39.9(2)
C(213)–C(214)–Fe(2)	69.5(3)	C(214)–Fe(2)–C(218)	120.3(2)
C(214)–Fe(2)–C(213)	41.0(2)	C(213)–Fe(2)–C(218)	106.9(3)
C(214)–Fe(2)–C(216)	164.5(2)	C(216)–Fe(2)–C(218)	67.0(3)
C(213)–Fe(2)–C(216)	153.7(2)	C(217)–Fe(2)–C(218)	40.6(2)
C(214)–Fe(2)–C(217)	154.1(3)	C(212)–Fe(2)–C(218)	125.3(3)
C(213)–Fe(2)–C(217)	118.4(3)	C(210)–Fe(2)–C(218)	154.8(2)
C(216)–Fe(2)–C(217)	40.1(2)	C(211)–Fe(2)–C(218)	162.4(3)
C(214)–Fe(2)–C(212)	67.6(2)	C(215)–Fe(2)–C(218)	66.5(3)
C(213)–Fe(2)–C(212)	40.04(19)	C(219)–Fe(2)–C(218)	38.8(3)
C(216)–C(215)–C(219)	106.8(6)	C(230)–C(231)–C(232)	122.5(5)
C(216)–C(215)–Fe(2)	69.1(4)	C(233)–C(232)–C(231)	119.4(6)
C(219)–C(215)–Fe(2)	69.8(4)	C(232)–C(233)–C(234)	121.0(6)
C(217)–C(216)–C(215)	108.9(6)	C(233)–C(234)–C(235)	119.4(6)
C(217)–C(216)–Fe(2)	70.1(3)	C(230)–C(235)–C(234)	121.0(6)
C(215)–C(216)–Fe(2)	70.9(4)	P(21)–C(236)–P(22)	109.3(2)
C(216)–C(217)–C(218)	106.9(6)	C(250)–P(22)–C(236)	103.5(2)
C(216)–C(217)–Fe(2)	69.9(4)	C(250)–P(22)–C(240)	103.5(2)
C(218)–C(217)–Fe(2)	71.0(4)	C(236)–P(22)–C(240)	102.0(2)
C(219)–C(218)–C(217)	107.9(6)	C(250)–P(22)–Co(22)	115.56(18)
C(219)–C(218)–Fe(2)	69.8(4)	C(236)–P(22)–Co(22)	110.98(17)
C(217)–C(218)–Fe(2)	68.4(4)	C(240)–P(22)–Co(22)	119.37(17)
C(218)–C(219)–C(215)	109.4(6)	C(241)–C(240)–C(245)	120.4(5)
C(218)–C(219)–Fe(2)	71.4(4)	C(241)–C(240)–P(22)	119.3(4)
C(215)–C(219)–Fe(2)	70.3(4)	C(245)–C(240)–P(22)	120.2(4)
C(220)–P(21)–C(236)	105.8(2)	C(240)–C(241)–C(242)	119.2(5)
C(220)–P(21)–C(230)	100.8(3)	C(243)–C(242)–C(241)	119.4(5)
C(236)–P(21)–C(230)	102.8(2)	C(242)–C(243)–C(244)	121.9(5)
C(220)–P(21)–Co(21)	119.55(19)	C(243)–C(244)–C(245)	119.4(5)
C(236)–P(21)–Co(21)	108.15(18)	C(240)–C(245)–C(244)	119.7(5)
C(230)–P(21)–Co(21)	117.98(19)	C(255)–C(250)–C(251)	116.5(5)
C(225)–C(220)–C(221)	117.2(5)	C(255)–C(250)–P(22)	122.8(4)
C(225)–C(220)–P(21)	123.4(4)	C(251)–C(250)–P(22)	120.1(4)
C(221)–C(220)–P(21)	119.4(4)	C(252)–C(251)–C(250)	120.8(5)
C(222)–C(221)–C(220)	121.6(5)	C(253)–C(252)–C(251)	120.1(6)
C(221)–C(222)–C(223)	120.7(5)	C(254)–C(253)–C(252)	120.1(6)
C(224)–C(223)–C(222)	119.6(5)	C(253)–C(254)–C(255)	120.4(6)
C(223)–C(224)–C(225)	119.4(6)	C(254)–C(255)–C(250)	122.1(5)
C(220)–C(225)–C(224)	121.5(5)	O(261)–C(261)–Co(21)	176.2(5)
C(231)–C(230)–C(235)	116.8(6)	O(262)–C(262)–Co(21)	176.0(5)
C(231)–C(230)–P(21)	124.8(4)	O(271)–C(271)–Co(22)	179.7(6)
C(235)–C(230)–P(21)	118.4(5)	O(272)–C(272)–Co(22)	175.2(6)

4.9. Preparation of **21**

A mixture of **18** (40 mg, 50 μmol), 2,6-dibromopyridine (4 mg, 20 μmol), bis(triphenylphosphine)palladium dichloride (2 mg, 3 μmol) and copper(I) iodide (2 mg, 10 μmol) in THF (10 ml) and diisopropylamine (30 ml) was refluxed for 24 h. The reaction solution was quenched with water, extracted with CH_2Cl_2, dried ($MgSO_4$) and concentrated under reduced pressure. Separation on silica gel, eluent 1:1 C_6H_{14}–CH_2Cl_2 gave one major band, which on workup gave **21** as a dark red powder (8 mg, 22%). Calc. for $C_{87}H_{71}Co_4N_3O_8P_4Si_2$: C, 62.10; H, 4.22; N, 2.49. Found: C, 62.99; H, 4.99; N, 2.58%. ^{1}H-NMR ($CDCl_3$): δ, 0.39 (s, 18H, $-CH_3$), 3.20 (q, 2H, $-CH_2$), 5.10 (q, 2H, $-CH_2$), 6.92 (m, 8H, Ar–H), 7.23 (s, 16H, Ar–H), 7.37 (t, 18H, Ar–H). IR (CH_2Cl_2, cm^{-1}): 2017, 1992, 1969 (ν_{CO}), 2055 ($\nu_{C\equiv C}$).

4.10. X-ray crystal structure

Crystal data for **8** are given in Table 3. Crystals were obtained from C_3H_6O–C_6H_{14} and a red brown rod was used for data collection. Data were collected on a Bruker SMART CCD diffractometer, processed using SMART and SAINT [27] and empirical absorption corrections applied using SADABS [27]. The structure was solved using SHELXS-97 [28] and refined by full-matrix least-squares on F^2 using SHELXL-97 [28] and TITAN-2000 [29]. The asymmetric unit of the orthorhombic unit cell contained two unique molecules. These were revealed in the chosen e-map of the direct methods solution. All non-hydrogen atoms were assigned anisotropic temperature factors, with hydrogen atoms included in calculated positions. At this stage of the refinement, the value of the Flack parameter [30] suggested the likelihood of racemic twinning. A check for the possibility of missing symmetry for the structure [31] was not successful. An overall scale factor was therefore refined using the twin model in SHELXL-97 [final value 0.406(7)] with subsequent reduction in the overall agreement factors. Final positional, thermal parameters and complete bond length and angle data are given in the Supporting Information (Tables 4–7).

5. Supplementary material

The material is available from the author on request.

Acknowledgements

We thank the Royal Society of New Zealand, Marsden Fund, for a Ph.D. scholarship (to B.D.) and financial support, J.M., J.M. and A.F. for advice and assistance, and Professor W.T. Robinson and Dr J. Wikaira (University of Canterbury) for collection of the crystallographic data.

References

[1] (a) V. Grosshenny, A. Harriman, M. Hissler, R. Ziessel, Platinum Metals Rev. 40 (1996) 26;
(b) P.G. Sames, G. Yahioglu, Chem. Soc. Rev. 23 (1994) 327.
[2] M. Hissler, W.B. Connick, D.K. Geiger, D. Lipa, R. Eisenberg, Inorg. Chem. 39 (2000) 447.
[3] A.K.A. Bunten, A.K. Kakkar, Macromolecules 29 (1996) 2885.
[4] (a) J. Okubo, H. Shinozaki, M. Kubota, T. Kobayashi, J. Electron Spectrosc. Relat. Phenom. 77 (1996) 267;
(b) S.C. Ng, I. Novak, X. You, W. Huang, J. Phys. Chem. Sect. A. 102 (1998) 904.
[5] I.R. Butler, C. Soucy-Breau, Can. J. Chem. 69 (1991) 1117.
[6] N.A. Agaltsova, I.R. Golding, A.M. Sladkov, V.V. Korshack, Vysokomol. Soldin. Ser. B. 14 (1972) 725.
[7] G.R. Newkome, D.L. Koppersmith, J. Org. Chem. 38 (1973) 4461.
[8] T. Lin, M.-F. Yang, C. Tsai, Y.S. Wen, J. Organomet. Chem. 564 (1998) 257.
[9] (a) B.H. Robinson, J. Simpson, in: M. Chanon, M. Juillard, J.C. Poite (Eds.), Paramagnetic Organometallic Species in Activation, Selectivity and Catalysis, Kluwer, Dordrecht, 1987, p. 357;
(b) C.M. Arewgoda, B.H. Robinson, J. Simpson, J Am. Chem. Soc. 105 (1983) 1893.
[10] C.J. McAdam, N.W. Duffy, B.H. Robinson, J. Simpson, Organometallics 15 (1996) 3935.
[11] (a) N.W. Duffy, C.J. McAdam, C. Nervi, D. Osella, M. Revera, B.H. Robinson, J. Simpson, Inorg. Chim. Acta 247 (1996) 99;
(b) N.W. Duffy, C.J. McAdam, B.H. Robinson, J. Simpson, J. Organomet. Chem. 565 (1998) 19.
[12] (a) N. Hagihara, Y. Kuroyama, K. Sonogashira, Synthesis (1980) 627;
(b) C.E. Castro, R.D. Stephens, J. Organomet. Chem. 28 (1963) 2163.
[13] D. Gregson, J.A.K. Howard, Acta Crystallogr. Sect. C 39 (1983) 1024.
[14] L.A. Hore, C.J. McAdam, J.L. Kerr, N.W. Duffy, B.H. Robinson, J. Simpson, Organometallics 19 (2000) 5039.
[15] (a) R.S. Dickson, P.J. Fraser, Adv. Organomet. Chem. 12 (1974) 323;
(b) J. Lewis, B. Lin, M.S. Khan, M.R.A. Al-Mandhary, P.R. Raithby, J. Organomet. Chem. 484 (1994) 161;
(c) C.J. McAdam, N.W. Duffy, B.H. Robinson, J. Simpson, Organometallics 15 (1996) 3935.
[16] C. Bianchini, P. Dapporto, A. Meli, J. Organomet. Chem. 174 (1979) 205.
[17] R.P. Aggarwal, N.G. Connelly, M.C. Crespo, B.J. Dunne, P.M. Hopkins, A.G. Orpen, J. Chem. Soc. Dalton Trans. (1992) 655.
[18] P.H. Bird, A.R. Fraser, D.N. Hall, Inorg. Chem. 16 (1977) 1023.
[19] S. Barlow, S.R. Marder, J. Chem. Soc. Chem. Commun. (2000) 1555.
[20] C.J. McAdam, A. Flood, B.H. Dana, unpublished results, Otago University.
[21] (a) M. Iyoda, T. Okabe, M. Katada, Y. Kuwatani, J. Organomet. Chem. 569 (1998) 225;
(b) M. Iyoda, T. Kondo, T. Okabe, H. Matsuyama, S. Sasaki, Y. Kuwatani, Chem. Lett. (1997) 35.
[22] C. Lapinte, T. Weyland, G. Frapper, M.J. Calhorda, J.-F Halet, L. Toupet, Organometallics 16 (1997) 2024.
[23] C.J. McAdam, M.Sc. Thesis, University of Otago, 1996.
[24] C.M. Arewgoda, B.H. Robinson, J. Simpson, J. Am. Chem. Soc. 105 (1983) 1893.

[25] I. Butler, Can. J. Chem. 69 (1991) 1117.
[26] E.C. Lisic, B.E. Hanson, Inorg. Chem. 25 (1986) 812.
[27] SMART (Control) and SAINT (Integration) software, Bruker, AXS, Madison WI, (1994); SADABS (correction for area detector data) Bruker AXS, Madison WI, 1997.
[28] (a) G.M. Sheldrick, SHELXS-96, A program for the solution of crystal structures from diffraction data, University of Göttingen, Germany, 1996;
(b) G.M. Sheldrick, SHELXL-97, A program for the refinement crystal structures, University of Göttingen, Germany, 1997.
[29] K.A. Hunter, J. Simpson, TITAN-2000. A molecular graphics program to aid structure solution and refinement with the SHELX suite of programs, University of Otago, New Zealand, 1999.
[30] H.D. Flack, Acta Crystallogr. Sect. A 39 (1983) 876.
[31] A.L. Spek, Acta Crystallogr. Sect. A 46 (1990) C34.